Laser Surface Modification of NiTi for Medical Applications

CHI HO NG

Department of Mechanical Engineering

University of Chester

2017

Laser Surface Modification of NiTi for Medical Applications

By

CHI Ho NG

Department of Mechanical Engineering

Thesis submitted in accordance with the requirements of the University of Chester for the degree of Master of Philosophy

November, 2017

Certificate of Originally

The material being presented for examination is my own work and has not been submitted for an award of this or another HEI except in minor particulars which are explicitly noted in the body of the thesis. Where research pertaining to the thesis was undertaken collaboratively, the nature and extent of my individual contribution has been explicit.

_____ (Signature)

Chi Ho Ng (Name of Candidate)

_____ (Date)

Abstract

Regarding the higher demand of the total joint replacement (TJR) and revision surgeries in recent years, an implant material should provide much longer lifetime without failure. Nickel titanium (NiTi) is the most popular shape memory alloy in the industry, especially in medical devices due to its unique mechanical properties such as pseudo-elasticity, damping capacity, shape memory and good biocompatibility. However, concerns of nickel ion release of this alloy still exist if it is implanted for a prolonged period of time. Nickel is well known for the possibility of causing allergic response and degeneration of muscle tissue as well as being carcinogenic for the human body beyond a certain threshold. Therefore, drastically improving the surface properties (e.g. wear resistance) of NiTi is a vital step for its adoption as orthopaedic implants.

To overcome the above-mentioned risks, different surface treatment techniques have been proposed and investigated, such as Physical Vapour Deposition (PVD), Chemical Vapour Deposition (CVD), ion implantation, plasma spraying, etc. Yet all of these techniques have similar limitations such as high treatment temperature, poor metallurgical bonding between coated film and substrate, and lower flexibility and efficiency. As a result, laser gas nitriding would be an ideal treatment method as it could overcome these drawbacks.

Moreover, the shape memory effect and pseudo-elasticity of NiTi from a reversible phase transformation between the martensitic phase and the austenitic phase are very sensitive to heat. Hence, NiTi implant is subjected to the following provisions of the thermo-mechanical treatment process, and this implant provides desired characteristics. It is important to suggest a surface treatment, which would not disturb the original build-in properties. As a result, the low-temperature methods for substrate have to be employed on the surface of NiTi. This present study aims to investigate the feasibility of applying diffusion laser gas nitriding technique to improve the wettability and wear resistance of NiTi as well as establish the optimization technique.

The current report summaries the result of laser nitrided NiTi by continuous-wave (CW) fibre laser in nitrogen environment. The microstructure, surface morphology, wettability, wear resistance of the coating layer has been analysed using scanning electron microscopy (SEM), X-ray diffractometry (XRD), sessile drop technique, 3-D profile measurement and reciprocating wear test. The resulting surface layer is free of cracks, and the wetting behaviour is better than the bare NiTi. The wear resistance of the optimised nitride sample with different

hatch patterns is also evaluated using reciprocating wear testing against ultra-high-molecular-weight polyethylene (UHMWPE) in Hanks' solution. The results indicate that the wear rates of the nitride samples and the UHMWPE counter-part were both significantly reduced. It is concluded that the diffusion laser gas nitriding is a potential low-temperature treatment technique to improve the surface properties of NiTi. This technique can be applied to a femoral head or a bone fixation plates with relatively large surface area and movable components.

Acknowledgements

I would like to express my sincere gratitude to my previous and current project supervisor Prof. Hau-Chung Man, Prof. Johnathan Lawrence, Prof. Nicholas Avis, Dr. David Waugh and Dr. Yu Shi for their patient guidance and genuine support in different aspects of this project. Their tireless leadership and inspiration help motivated me in completing this MPhil programme. I have gained many unforgettable experiences in both United Kingdom and Hong Kong which will indefinitely enrich my life.

I would like to thank Dr. Chi-Wai Chan and Dr. Fai-Tsun Cheng who provided me extra knowledge and care in my research, in particular Dr. Chi-Wai Chan who provided me invaluable opportunity to be a visiting research associate at Queen's University Belfast, UK. I would also like to extend this thanks to his team and other colleagues in Belfast for their continuous guidance in the laser experiment. Their training provided me with proficient skills to confidently cope with various instruments.

I am also indebted to Dr. James Nicholson, Mr. Rico Cheung, Mr. S.Y. Lau and Mr. T.W. Chan for their technical support and preparation of specimens in UK and HK.

The funding from University of Chester, UK for this international studentship is gratefully acknowledged. This research work was also partly supported by the visiting research associateship which was provided by the School of Mechanical and Aerospace Engineering, Queen's University, Belfast, UK, and by the Hong Kong Polytechnic University, Hong Kong Special Administration Region, China research (Grant Nos. G-YK36 and G-YM75).

Last but not least, I would like to offer thank you to my family and friends in Hong Kong. Without their emotional support and encouragement, I could not complete my MPhil programme successfully.

List of Publications

Journal Papers

1. **Chi-Ho Ng**, Chi-Wai Chan, Hau-Chung Man, David Waugh, Jonathan Lawrence, "Modifications of surface properties of beta Ti by laser gas diffusion nitriding", Journal of Laser Applications, Vol. 28 (2), 2016, 022505
2. **C.H. Ng**, C.W. Chan, H.C. Man, D.G. Waugh, J. Lawrence, "NiTi shape memory alloy with enhanced wear performance by laser selective area nitriding for orthopaedic applications," *Surface and Coatings Technology,* vol. 309, pp. 1015-1022, 2017.

Conference Proceedings/Posters:

1. **Chi-Ho Ng**, Jonathan Lawrence, Graham Smith, David Waugh, Chi-Wai Chan, H.C. Man, "Process Optimization for Laser Gas Nitriding of Shape Memory NiTi alloys", UKSAF Summer Meeting, July 1, 2015, Chester, UK (Poster)
2. **Chi-Ho Ng**, Chi-Wai Chan, H.C. Man, David Waugh, Jonathan Lawrence, "Modifications of Surface Properties of Beta Ti by Laser Surface Treatment", Laser Materials Processing Conference, 34th International Congress on Applications of Laser & Electro-optics (ICALEO), October 18-22, 2015, Atlanta, USA, paper no. 203, (Oral Presentation)
3. **Chi-Ho Ng**, Chi-Wai Chan, Hau-Chung Man, David Waugh, Jonathan Lawrence, Graham Smith, "Novel Laser Technology to Enhance the Wear Resistance of Shape Memory NiTi Alloy for Total Joint Replacement Applications", Journey through Science Day, December 14, 2015, New York, USA (Poster)

Table of Contents

List of Figure Captions

List of Table Contents

List of Equations

1. Introduction

1.1. Background of Study

People all over the world are demanding better quality of life. Thus, there is a growing demand of replacement and revision surgeries in recent years. Total joint replacement (TJR) is therefore more essential and critical in orthopaedics. In 2012, over 98,000 total hip replacements (THRs) were performed in the UK, more than 1 in 10 of these were revision THRs [1]. According to the data collected on TJR surgery, it is estimated that by the end of 2030, the demand of THRs will rise by 174% and total knee arthroplasties is projected to grow by 673% from the present rate [2]. Moreover, the hip or knee prostheses are expected to increase its longevity in order to reduce the possibilities of future revision surgery as revision surgery is very expensive and the results are usually less satisfactory than the primary surgical treatment [3].

Metallic implants are recommended for orthopaedic implants, especially for load bearing application, because of their excellent mechanical properties compared with ceramic and polymer. The metallic materials possess appropriate combination of high strength and low modulus, high fatigue and wear resistance, high ductility and be without cytotoxicity [4]. Therefore, metallic implants are proposed in such application.

Although the metallic material is an ideal candidate for implant material, there are still some drawbacks after long term use, such as malpositioning, instability, periprosthetic fracture (i.e. a broken bone occurred around the implant components of TJRs) and infection (i.e. bacteria exists during implant surgery or post-surgery without appropriate hygiene) [3, 5, 6]. The debris generated between the implant movement will affect the proper function of implants giving to loosening and components mismatch, and subsequently create a side effect to the surrounding body tissues and bones. These debris also provide a source for bacteria growth which will increase the rate of infection. With this scenario, improvement to metallic implants is necessary in extending the implants lifetime so that the number of revision surgeries is kept at a minimum.

The wear behaviour of the implant materials is a concern in implants, because of its subsequent side effect to the patient. The process of wear in TJR can generate wear debris that causes TJR aseptic loosening and implant failure including femoral component [7, 8].

Worse still, the patient may be infected by wear debris. With regards to the above-mentioned issues, the design engineer need to strike a balance between different properties and considerations, including processing time and cost, material surface chemistry, mechanical properties, corrosion resistance and biocompatibility etc. In this connection, surface modification provides an alternative to enhance surface and mechanical properties without altering substrate bulk properties.

1.2. Nickel Titanium as an Implant Material

Nickel Titanium (NiTi) shape memory alloy is a stoichiometric compound which is a solid solution with 55 w.t. % of Ni and 45 w.t. of Ti [9]. Comparing to conventional metallic materials, such as stainless steels and Ti-6Al-4V, the shape memory effect, super-elasticity and good biocompatibility of the NiTi are the attractive mechanical properties for this promising material in commercial medical implants [10, 11, 12, 13, 14]. Especially the shape memory effect, its alloy can restore the original shape of a deformed sample by heating it up to a specific temperature (i.e. transformation temperature). This phenomenon is named as 'thermoelastic martensitic transformation'. The brief process is that cool austenite (high temperature phase in NiTi) to form twinned martensite (low temperature phase), then deform/untwine martensite by external force, afterwards heat to revert to austenite (original shape). It is known as shape memory effect and the detail will be discussed in section 2.2.1. Apart from the shape memory properties, NiTi alloy also has excellent corrosion resistance, wear resistance and mechanical damping capacity [10, 11, 12, 13, 14].

Stress shielding is related to the redistribution of load and consequently the reduction of the bone density, which results in the removal of stress on the living bone by the nearby implant, for example, the metal components in the total hip replacement [15]. Referring to Wolff's law, the human or animal bone is ready to remodel under load, thus, the loading on a bone is decreasing, the bone is trend to reduce the density and weaken due to no stimulus for the remodelling in order to maintain the bone mass. The great mismatch in Young's modulus between metallic materials and the surrounding bone results in stress shielding. In comparison with the Young's modulus of Co-Cr alloys (200-220 GPa) and stainless steel (approximately 200 GPa), NiTi SMAs have lower Young's modulus (e.g. 70-110 GPa for B2 austenite and 29-69 GPa for the B19' martensite), which may reduce the stress shielding effect if they are used as orthopaedic implant [16]. As a result, this alloy may be applied for

the manufacturing of equipment and devices used for medical application in orthopaedics and dentistry, such as stents, bone anchors, fixation nails, bone staples, compression plates, orthodontic arch-wires, dental root implants and adjustable brackets [17, 18].

Although NiTi is not currently used as the major component in TJR implants, it has been recommended as a material with high potential for such orthopaedic applications [19] among 10 metallic materials in current use (e.g. Ti-6Al-4V and CoCr) and potential materials. This recommendation based on a holistic consideration to judge the material's possibility for the implantation. For example, factors including density, tensile strength, Young's modulus, elongation, wear resistance and osseointegration. However, similar to other Ti alloys, there is a concern of the relatively poor wear properties, especially for NiTi alloys with high Ni content (i.e. Ni ion release may cause toxicity, asthma, allergic and immune sensitizing [20, 21]). In potential orthopaedic application where they are used as femoral head against with plastic liner [22, 23], wearing of NiTi will produce debris which might invoke inflammatory and immunological responses [24]. To avoid this, surface modification of NiTi may be effective in keeping the bulk properties while improving the wear performance by forming a protective layer (e.g. TiN) to prevent Ni ion from being released.

1.3. Motivation of Current Study

1.3.1. Need of Surface Modification

The wear debris generation after a long term wearing in the movable component is a major factor affecting the performance of NiTi implants. The high concentration of nickel in the NiTi alloy also has hindered its use for long term implantation. Some studies reported that the high Ni content alloys might release Ni ions in an aggressive physiological in vivo environment, and the release of nickel may induce toxic and allergic response to body tissues [18, 25, 26, 27]. The subsequent release of Ni ions into the body system is a fatal issue for long term application of this alloy in the human body, and currently poses a challenge to use NiTi for long-term implantation. Given the excellent properties of NiTi related to its high Ni content, significantly reducing Ni content inside the bulk substrate is therefore non-negotiable. It will be most advantageous if NiTi surface could be modified without sacrificing the bulk composition, to reduce surface nickel content, and improve the wear resistance and biocompatible properties of the surface.

1.3.2. Importance of Low-Temperature and Non-Roughening Treatment

Various surface modification methods (e.g. Physical vapor deposition (PVD), plasma immersion ion implantation (PIII), physical treatment and hydrothermal deposition of calcium phosphate coating) are available in literature [28, 29, 30, 31] for enhancing the wear resistance and biocompatibility of metallic implants, such as titanium and stainless steel implants. Those methods were successfully performed, for example, PVD coated 316L stainless steel showed significant enhancement on both wear and corrosive condition in simulated body fluid; PIII treated samples demonstrated better blood compatibility and antibacterial property. However, most of these methods may not be an ideal solution for NiTi although they work well for other metallic materials. NiTi shape memory alloys exhibit shape memory effect and pseudoelasticity from a reversible phase transformation between a low-temperature phase (martensite) and a high-temperature phase (austenite) [32]. It is well known that the transformation features and the mechanical properties of NiTi are very sensitive to heat (e.g. temperature above 400 °C). When the temperature is too high, phase change may take place, resulting in an undesirable effect on the mechanical properties of NiTi implants. It is important that any surface modification and sterilization process should avoid undergoing at high substrate bulk temperature, otherwise the built-in properties of the NiTi implants may be affected. High temperature treatment will cause the surface of NiTi to melt and subsequently re-solidify after cooling. More importantly, non-roughening treatment, a low temperature surface modification method, is necessary, so as to avoid the occurrence of undesirable roughened surface that may reduce the wear resistance. The roughened surface requires post-treatment as well, which may increase manufacturing cost. For non-roughening treatment, the process should be controllable to reduce the risk of affecting the built-in properties and surface feature of NiTi implants. Not only does it improve the mechanical properties of NiTi, but it also sheds lights on scaling up the lab-based research to industrial application.

1.3.3. Surface Modification – Laser Gas Nitriding

Laser is accepted as an effective tool to modify the surface appearance or composition of a material in order to improve their mechanical and chemical properties as well as biocompatibility. Conventional Laser Gas Nitriding (LGN) of titanium alloys was initiated by Katayama et al in 1983 [33]. LGN is an efficient technique offering accurate spatial control of

surface treatment without any undesired heating of the substrate. It is chemically clean and capable for remote non-contact processing. It is also relatively easy to automate. Conventional LGN usually forms an atomically intermixed layer between metallic substrate and coating, resulting in high bonding strength [34]. Initial research in this field focused on the microstructure characterization and mechanical behaviour of nitride surface. Hoeche et al [35] discussed the cracking problem observed in the LGN of titanium. They concluded that cracking is a major concern, especially on thick layers' formation. Schaaf et al [36] studied the wear resistance of the laser nitrided titanium alloys and reported that the abrasive wear resistance of Ti-6Al-4V could only be improved if the thick layer exhibits hardness of 800 HV or above. The friction coefficient and the mass loss under sliding wear conditions can be both minimized effectively by continuous-wave (CW) laser nitriding [36]. Nevertheless, conventional LGN involves surface melting and roughening in a nitrogen atmosphere. Thus, the post surface treatment is inevitably required. Alternatively, diffusion laser gas nitriding (DLGN) method without surface melting and roughening was developed [37]. The results showed that the Titanium Nitride (TiN) on the surface of the Ti alloy (i.e. Ti-6Al-4V) could significantly reduce the wear debris from the bulk material to the surrounding. However, there is no any investigation of non-roughened homogenous TiN fabrication by the DLGN on NiTi surface. It is believed that the thin and homogenous TiN could improve the hardness, wear resistance and wettability on Ti and Ti alloys. As a result, a comprehensive analytical study on NiTi by DLGN is necessary.

1.4. Aims and Objectives

As introduced previously, on one hand, proper surface treatment, promotes wear resistance, on the other hand, it reduces ions release rate that enhance the safety of metallic implants in the long run. Moreover, in the implant fixation (i.e. involves the surgery of implants implementation for repairing a bone or a joint), bone-cell adherence also is the another concern and affects the successful rate of implants in early stage. It has been well researched that bone cell adherence is associated with the surface topography, chemical composition and roughness [30, 38, 39, 40]. So these properties of the implants should be extensively investigated which ensure the wear resistance and biocompatibility of implant materials in long term use by applying suitable surface treatment. In particular, the debris generated from the implant movement has high potential to affect both wear and biological

responses of implants, so wear improvement and debris reduction combined with analysis of surface topography, chemistry and roughness is the first priority to be studied in current case. As a result, the cell adherence and biological performance will not be included in the present study.

Existing studies in this area are based on the conventional laser gas nitriding (CLGN) method by which only a single parameter is varied in each run with other parameters being kept constant. It is ineffective to understand the laser parameters because the interactions between each other are normally neglected. Because of this, there is a knowledge gap between study of design of experiments (e.g. Taguchi method) and optimisation of the laser parameters with their interactions on the surface properties. The aim of the study is to understand the relationship between different laser parameters and their interactions on the surface properties. Besides, coating with the process optimization, coverage quantification, surface morphology, wear behaviour as well as wettability of nitriding surface will also be studied.

The following specific objectives are pursued:

1. To investigate the relationship of laser processing parameters upon the geometric characteristics of the single track of TiN on NiTi
2. To study the surface coverage of laser track after nitriding of NiTi after process optimization
3. To create full of TiN surface and different hatch patterns TiN surface on the NiTi and examine the wear resistance of these specimens
4. To study the wettability of bare and nitrided NiTi by eliminating the surface roughness effect in wetting property

1.5. Research Significance and Value

Good mechanical properties and biocompatibility of NiTi make them favourable in various areas of application, such as orthopaedic and dentistry applications. NiTi can further be applied into other industries, e.g. aerospace, if its tribological performance and wetting properties can be better understood and improved. Therefore, the results of the current research may facilitate the nitrided NiTi for better cell adhesion and its biological responses inside the human body. The significance of this research includes:

1. Contribution to the development of an optimum laser nitriding process of NiTi
2. Improvement of surface properties of NiTi for potential application such as femoral component in hip/knee implant
3. Determination of the percentage of nitrided area on the NiTi surface by Image analysis
4. More comprehensive understanding of the wetting properties of NiTi by changing surface composition only

2. Literature Review

2.1. Introduction

Inserting biomaterials as an implant into the human body can facilitate better biological and mechanical functioning, which can improve the quality of life of patients. Due to a wide variety of biomedical applications, the implant should withstand under higher mechanical load and also has a desirable long-term biological response with the surrounding tissues. The part for the load bearing application is mainly controlled by the mechanical properties of the implant materials whereas the interaction between the surrounding tissue and implants is affected by the surface properties of the implant materials [20, 30, 38]. The implant surface influences the wettability, and subsequently affects the interaction and absorption of different proteins which in order to govern the cell adhesion and behaviour. In general, the overall reaction relating the human body to an implant is a complex systematic process that includes many aspects, namely surface morphology, surface chemistry, surface free energy, biodegradation, implant movement and surgical aspects. Moreover, the relative corrosive human body fluid and the high sensitivity of the human body to some dissolved metal ions (i.e. Ni and V) prohibit the materials to be a promising implant materials. Nowadays, the current used metallic biomaterials which can be employed in medical applications as implants are CoCr alloy, stainless steel, NiTi shape memory alloy, titanium and its alloys. In this chapter, the mechanical properties, surface properties and the medical applications of NiTi shape memory alloy are reviewed. In addition, the problems including the wear behaviour are scrutinized and the possible treatment methods are illustrated. The wear behaviour and surface roughness of the Ti and its alloys by the laser nitriding are studied at the end of the reviewing of literatures

2.2. Metallic Materials for Hard Tissue Replacement

Metallic materials has emerged as an important biomaterial for fabricating implantable devices, such as replacement implants in human joints, orthodontic arch wires and intravascular stents, due to its outstanding mechanical performances that may not be found in the polymer and ceramic [14, 41]. Regarding their excellent mechanical properties, the most commonly used metallic materials for medical application include Ti, Ti alloys, NiTi shape memory alloys, stainless steels and cobalt chromium alloys for bone plate, hip and knee

replacement. In particular, NiTi shape memory alloy is an attractive biomaterial in the biomedical applications due to its shape memory effect.

2.2.1. NiTi Shape Memory Alloys

Nickel Titanium (NiTi) shape memory alloy has been increasingly used in the medical devices industry as their specific characteristics [10, 11]. NiTi alloy is a stoichiometric compound which is a solid solution with 55 w.t. % of Ni and 45 w.t. % of Ti [9]. The shape memory effect, super-elasticity and good biocompatibility of the NiTi are the attractive concerns in commercial medical implants [10, 11, 12, 13]. Apart from the shape memory properties, NiTi alloy also has excellent corrosion resistance and mechanical damping capacity. For the shape memory effect, it is a phenomenon such that a specimen is deformed below martensite finish temperature (Mf) or at temperatures between Mf and austenite start temperature (As). Upon to a temperature above Austenite finish temperature (Af), the NiTi specimen may regain its original shape by reverse transformation. The shape of the NiTi alloys does not change due to the transformation occurs in a self-accommodating manner. When the external stress exists, the twin boundaries move to accommodate the applied stress. Furthermore, if the stress is high enough, it will become a single variant of martensite and changes into the twin orientation by shearing to create a large twinning shear strain. A subsequent heating is applied to the specimen and the temperature is above Af, reverse transformation is likely to occur, and the crystallographically reversible, the original shape will be rewarded. This is the mechanism related to shape memory effect. Besides the shape memory effect, super-elasticity is one of the attractive properties of NiTi alloys. When the NiTi alloys is in its austenite phase, a highly elastic behaviour is exhibited. This allows the material to deform up to 7 % which the common alloys are far below 1 % in the elastic strain [42]. Super-elastic NiTi can be strained several times more than ordinary metal alloys without being plastically deformed, which reflects its rubber-like behaviour [43]. In addition, for the elastic modulus, the NiTi shape memory alloys can exhibit as low as 30 GPa in the martensitic state (The elastic modulus of Bone: 10 – 40 GPa [20]) which can get rid of stress shielding effect. With the above-mentioned properties about NiTi shape memory alloys, they are more appropriate than other metallic material in load-bearing applications.

2.2.1.1. Orthopaedic Applications

The NiTi shape memory alloys have been widely used in orthopaedic as its well-known shape memory effect and outstanding mechanical performances that may not be found in titanium and stainless steels [20, 44, 45]. For example, the spinal vertebra spacer is one of devices applied for orthopaedic, as shown in Fig. 1 [46]. This spacer is inserted between two vertebrae which can avoid any traumatic motion during the healing process depending on the local reinforcement. The shape memory spacer, can sustain a constant load in the certain position of a patient and avoid some degree of motion [47]. Normally, it is used in the treatment of scoliosis [48]. As shown in Fig. 1, it can be observed that the left side in part B, the spacer is in the martensitic stat, and on the other side, the spacer is in its original shape which is related to the recovery by the pseudo-elastic phenomenon.

According to the fractured bone healing, one most expected application is the recovery of the bones. The bone plates, which are made from NiTi shape memory alloys, are primarily used in situations where a cast cannot be applied to the injured area, such as jaw and eye socket. The aim is to maintain the original alignment of the bone and allow a better tissue proliferation. In accordance with the shape memory effect, when the suitable temperature is applied on these bone plates, these bone plates tend to recover their former shape while a constant force exerts to join parts separated by fractures, helping with the healing process [48]. Fig. 2 shows the prototype designed for the above-mentioned application.

It is worth to note that one more interesting application is the porous shape memory alloy. It has a great potential in orthopaedic implants with regard to their porosity that allows the flow of body fluids from outside to inside the bone. It can enhance the successful rate of treatment and also helps the fixation of the implants [49].

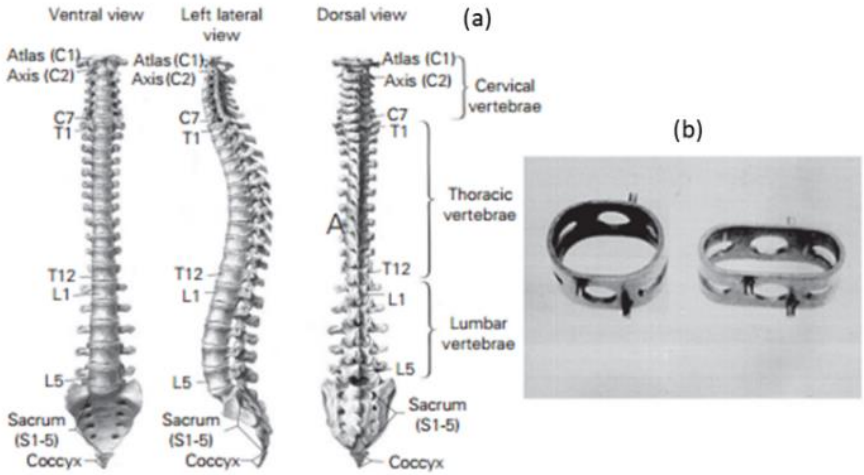

Figure 1 The schematic diagram of spinal vertebrae (a) and shape memory spacers (b) [46]

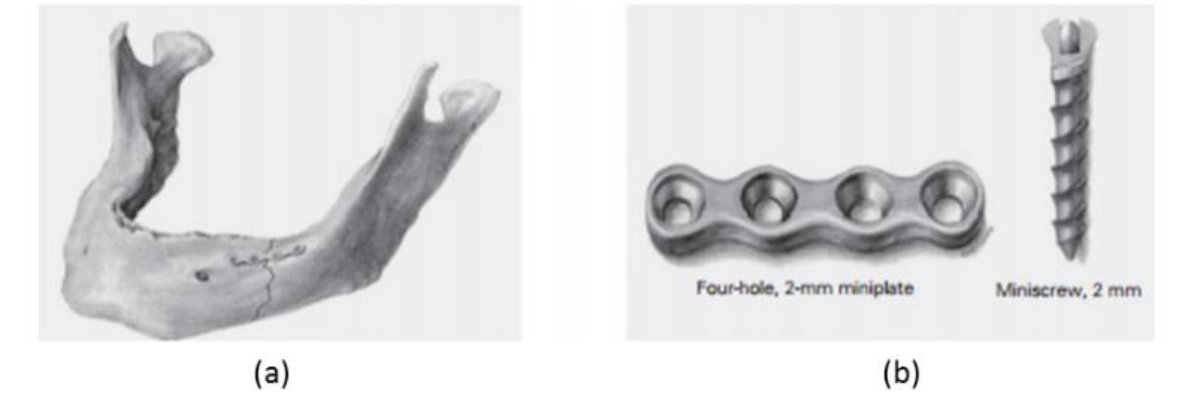

Figure 2 Shape memory bone plates, (a) plates fixed upon a human jaw, (b) Detail of the plate and the screw [46]

2.3. Problems Associated with Biomaterials used in Medical applications

On the basis of the attractive mechanical properties and corrosion resistance, Ti and its alloys become ideal candidates used in medical applications since last mid-century and NiTi SMA has been widely developed as metallic biomaterial for medical purpose [50]. For the long-term reliability of implantation, a problem associated with biomaterials (e.g. Ti and NiTi), such as long-term wear and debris generation, is discussed in following sections in details. Laboratory-scale performance testing and measurement of biomaterial properties are also illustrated.

2.3.1. Long-Term Wear and Debris Generation

Wear is a technical term and is defined as the continuous removal of material with progressive generation of wear debris. The relative motion is the result obtained between

two opposing surfaces under certain loading [51]. It is perhaps the most important aspect of biomaterials which used in TJRs and for this reason is attracting considerable attention at the present time. There are five main types of wear mechanisms, that is, adhesion, abrasion, fatigue, corrosion and erosion [52, 53]. Moreover, delamination, penetration, pitting, fretting and cavitation which are descriptive of the appearance of the worn surface [54].

For example, adhesion is occurred when two surfaces are pressed together under loading to form surface bonds; sufficient relative motion causes the material pulling away from one or two of the surfaces, which often happens on the weaker material surface. In the abrasion situation, the asperities or protuberances on the harder surface plough through the softer surface, the result is to remove the material from the softer surface. There are two types of abrasive wear, such as two-body and three-body abrasive wear. For the two-body wear, it is resulting from the hard protuberances on the harder surface sliding between two contact surfaces; On the other hand, three-body wear is caused by the hard particles being free slid and rolled between two contact surfaces. For the fatigue wear, it is induced by the applied local stress once it has exceeded the fatigue strength of a material subjected to a period of loading cycles, the material will be thus failed to release material from the surface. Chemical or electrochemical reactions involved in the wear process is known to be corrosive wear. Erosive wear is defined as the loss of material from a solid surface in contact with a fluid containing solid particles during relative motion.

In many cases, two or more wear mechanisms could be mutually inclusive. For example, adhesive wear may release wear particles, subsequently induce an abrasive action. In the case of polymers, adhesion, abrasion and fatigue wear could be existed simultaneously to the overall wear process [54]. Abrasive wear could be minimised and reduced by creating a smooth surface on the harder material or a better sealing to control abrasive particles release. For the fatigue wear, it could be managed by material stress levels in the design process and the frequency of stress reversals. The careful material selection or environmental selection can reduce harmful chemical reactions to minimise corrosive wear. It should be mentioned that adhesive wear could be the least manageable wear mechanism in joint tribology, because the adhesion is easily formed between two contact surfaces in relative motion [53] and therefore, this wear mechanism is most of concern in joint tribology.

2.4. Wear Testing and Measurements of Biomaterials

The wear rate of the bearing biomaterials in the medical devices is a crucial parameter to determine the life of the implants. Therefore, it is important to accurately measure the wear rate of proposed designs for medical components and ensure that the certain designs will be satisfied [54, 55]. Moreover, the wear tests can help to understand the basic wear mechanisms under certain circumstances. There are several procedures to evaluate wear performance, such as testing components in joint simulators, laboratory testing of biomaterials under controlled situations and monitoring the performance etc.

Direct measurements of the prostheses under tribology condition can be clinically performed in vivo, for instance, by the radiographic measurements or the measurement of dimensional changes in explanted prostheses [53]. However, due to creep effect, it is difficult to distinguish the wear and deformation for each measurement.

The long test time of the bearing assembly and the expensive test procedure of the total joint displacement simulator, a simple laboratory test is attractive in the case of basic information of the wear mechanism between the two surfaces [54]. The main idea of laboratory wear testing is to utilise the known applied load, the known sliding materials and the known velocity with controlled circumstance to record the amount of material removal rate under wear condition. Laboratory equipment was identified as a screening device for studying the wear behaviour of prosthetic biomaterials to develop an integrated wear process and to further understand the level of wear in order to develop joint designs in the future. Commonly used screening devices for the wear process may be pin-on-ring, pin-on-disc and reciprocating pin-on-plate testing machines. Pin-on-disc screening device is most popular due to stable operating conditions and good operating conditions. However, in the Pin-on-disc test, only high-speed and unidirectional motion are used, so this screening test failed to investigate the characteristics of the joint movement as it is a reciprocating motion. The reciprocating pin-on-plate screening device can be a good reflection of the lower limb bearing joints encountered at this situation [53]. Thus, the reciprocating pin-on-plate screening test can provide more realistic quantitative data to estimate the tribological performance of total hip and knee arthroplasty in vivo.

Tribo-pairs of implant materials are often recorded in different ways in the laboratory scale, such as material weight loss measurement, the collection of wear debris and optical measurement of surface topography changes. In general, by using these recording techniques to evaluate the wear performance, it can be seen that increase in normal load, sliding distance and hardness of softer counter-part may result in an increase in wear rate [54]. If the average contact stress between two counter-parts is not high, the wear rate of the polymer and metallic counter-part can be given with fair accuracy by the following equation [56, 57]:

Equation 1 Archard Equation

$$k_i = \frac{V}{F \times S}$$

Where k_i is the wear factor (or the specific wear rate coefficient) (mm^3/Nm). Index i identifies the surface considered. F is the normal load (N), S is the total sliding distance (m), V is the wear volume of material (mm^3). The wear factor is an indication of the wear rate with given combination of materials, and it is usually used for comparative purposes to study the wear properties of potential prosthetic materials [53].

The conventional wear screening devices may excessively simplify the motion/loading configurations, and the low wear rate of UHMWPE may be attributed to the liner motion of the conventional wear testing devices [53]. Therefore, the linear motion of the conventional wear tester may underestimate the wear factors of the joint simulators and clinical results, and provide some inappropriate wear rate rankings for the relative components. From the literature [58, 59], the higher clinical wear rates in UHMWPE counter-part may ascribe to the multidirectional motion of the human joint. Consequently, the reliable wear rate of polymer and metallic biomaterials should be comparable to that of clinical wear rates, and should be examined in the multi-directional motion of the wear screening devices or joint simulator [58, 59].

In the wear mechanism between two contact surfaces, a frictional force is always presented that opposes the motion of an object [51]. Sliding and rolling are the two classes of relative motion in friction. The difference between rolling and sliding is remarkable, but cannot be mutually exclusive because almost all rolling motion involves some sliding motion. In the ideal case of rolling and sliding motion, a tangential force (F) is required to slide the

upper object over the stationary counter-part. The ratio between this force and the applied normal load (P) is defined as the coefficient of friction (μ) [60]:

Equation 2 Coefficient of friction equation

$$\mu = \frac{F}{P}$$

The friction force is directly proportional to the applied normal load for most metallic and ceramic materials under lubricated and unlubricated sliding conditions. However, polymeric materials do not always follow the same condition happened in both metallic and ceramic materials. Generally speaking, the frictional force is usually greater in the initiation of sliding than in the maintenance of sliding, hence, the coefficient of dynamic friction (μ_k) is lower than the coefficient of static friction (μ_s). Once the static friction (μ_s) is established during sliding, it is found that static friction is nearly independent of sliding velocity for a wide range of sliding. Moreover, dynamic friction (μ_k) may fall with increasing velocity in the very high speed sliding.

In the real life, for example, in the natural hip joints sliding motion, the coefficient of friction is around 0.005 [61]. The data of the coefficient of friction can give a help to illustrate the wear behaviour between two contact surfaces in total joints replacement. Throughout tracking frictional force data and identifying the range of the coefficient of friction, it can make a reasonable prediction of the duration of the use of artificial joints.

2.5. Laser Nitriding of Titanium and its Alloys

The chemical cleanliness, automated control and fast processing times have been identified as the reason of surface modification of biomaterials by laser nitriding in terms of effectiveness and reliability. Another advantages in the view of material science of laser nitriding is that the titanium nitride layer is metallurgically bonded with substrate. In other words, this method could increase the bonding strength between substrate and nitride layer. Hence, this method could minimize the possibility of peeling off nitride layer. In this section, laser nitriding was mainly discussed with respect to the principles and major parameters of the nitriding process as well as the mechanical properties of the nitrided surface.

2.5.1. Principles of Laser Gas Nitriding

Laser gas nitriding is one of the category in the area of laser surface alloying. It normally involves a surface melting and roughening of the treated samples with the nitride layer fabricated on the surface. The nitride layer is tightly bonded with the substrate and provide a superior protection to the metallic materials in terms of wear and corrosion resistance. For the better understanding of the nitriding process to facilitate well in mechanical improvement, the individual physical and chemical interaction within the process by implementing different laser parameters should be clearly identified. However, the entire process of laser nitriding is difficult to clarify due to the complexity of its interaction in various scientific background (e.g. chemical reaction between gas and metallic materials, materials' physical properties) [28, 29].

In general, the nitriding process is dominated by the local heating from the laser irradiation and subsequently rising surface temperature. This determines the nitrogen intake for TiN fabrication and the surface condition after the treatment. The lower heat input, the reaction rate between nitrogen and metal surface may be reduced. The higher heat input, the over-saturated TiN surface may be formed and this results in roughening surface and highly brittle surface feature. Therefore, various laser processing parameters should be included in the systematic approach to understand the influences between each processing parameters, subsequently pave a way to improve the heating and melting effects and even the sensitivity of evaporation on the sample surface [35]. For the purpose of better understanding the laser nitriding process, it is necessary to clarify and quantify the influences from different processing parameters to the coatings and their properties [35].

2.5.2. Process Control and Optimization

In order to optimise the nitriding process of LGN research, extensive experiences in the laser processing will be necessary. First of all, the laser processing parameters should be analysed to understand the dependency on the process control, such as the beam size, and the most important processing parameters and the range of parameter values that need to be determined or estimated. The laser power density may be the most important parameter in the laser material processing, and can be varied by the focal length and the laser spot size [35]. The pulsed and continues wave modes are also key factors in determining the laser materials processing. For the continuous-wave (CW) mode, the scanning velocity is an

important parameter in the process whereas the pulse frequency is decisive for the pulsed mode [35]. Other parameters corresponding to the optimisation process are the gas pressure and gas flow [35]. These two parameters indirectly determine the surface quality and morphology.

In addition, it has to be noted that another factor affecting the nitriding process is the material itself. In the processing, thermodynamic and mechanical properties of the irradiated material are gradually changed, and the mechanism is significantly affected by the changes in the accumulation state [35]. Moreover, the size of the work-piece, especially the thickness, strongly affects the cooling rate that controls the solidification process and the subsequent surface quality [35]. The similar process, such as laser welding, involves heating and cooling, which preheating the substrate before processing to reduce residual stresses in the welded thick section. This idea can be applied to laser nitriding as well and the effect of the preheating was proved to be remarkable in the LGN titanium alloys [62].

For the optimisation of laser nitriding, it was rarely found in the literatures that most of the researchers focused on the microstructure and mechanical behaviour of the laser treated samples [35, 62]. For example, Perez et al [62] demonstrated the limited laser processing parameters for optimisation with the combination of the laser power and the scanning speed. The quality of the laser nitrided layer was found that free of porosity and crack [62]. In order to better understand the optimisation of laser nitriding, it is more important that the optimisation process should be based on a quantitative basis beyond the qualitative foundation for laser nitriding process optimisation.

2.5.3. Cracks in Laser Gas Nitriding

The cracks are rarely avoided in most of the metallic materials during laser nitriding. Therefore, the approaches to eliminate the cracks have been reported. Liu [63] found that the cracks formed on the nitrided surfaces of Ti-6Al-4V alloys were divided into two categories: the first type was the macro-cracks induced by the accumulation of residual stresses due to surface melting; the second type was the micro-cracks ascribed to the inherent brittleness of Titanium Nitride (TiN). The proper selection of laser parameters and condition, such as gas environment, energy level and scanning speed, were thus suggested in his work to avoid cracks formed in the nitrided surface.

Moreover, Hoche et al [35] found that cracks formed in thick nitride surface were always a critical issue. The reduction of nitrogen content in the nitriding processing was an effective way to prevent the cracks formed, however, this approach resulted in a significant reduction in hardness and wear resistance, which were not expected. An alternative has been published to use diode laser, the authors found that the cracks were only eliminated once the work-piece was preheated to 500 °C , which was not sensitive to the nitrogen content applied [62]. However, this result was in conflict with most of previous studies in the laser nitriding process [64, 65, 66]. The reason might be the author using thick work-piece or performing the nitriding in different environment. Therefore, the effect of preheating the work-piece before the nitriding process has to be further elucidated in experiment.

2.5.4. Phase Transformations of Laser Nitrided Surface

Phase transformations or phase transition is a change in a feature of a physical system, often involving the energy absorption (e.g. heat) from the system, resulting in transitions between solid, liquid and gaseous states of matter. The laser gas nitriding method can be simply explained as the surface melting results in the surface of titanium and its alloys. As the surface melting is involved, this means that a phase change is likely existed on the surface of titanium and its alloys from the solid state to the liquid state during laser irradiation, and the liquid state of titanium and its alloys react with the surrounding gases to form new compounds (e.g. TiO_2, TiN). If the cooling rate is sufficiently fast (i.e. depending on the process parameters and the size of the sample), and the nitrogen content is under 6.2 At. % inside the titanium and its alloys, a martensitic transformation (ά-Ti) could be obtained.

The hardness is an indicator to indirectly illustrate the phase transformation inside the materials. For example, if the hardness is reduced from the top of surface layer to the substrate, this means that the phase on the surface is completely different from that in the substrate [67, 68]. In the case of nitriding samples, due to the presence of TiN, a higher hardness occurs on the surface, the hardness is decreased from the top (e.g. TiN) of the sample to the ά Ti-N solid solution matrix area (e.g. TiN dendrites) and the substrate (e.g. Ti). Between melt zone and heat affected zone, only the ά Ti-N solid solution exists, and the lower hardness level reflects lack of TiN, this means that the phase between melt zone and heat affected zone is not the same [67, 68].

Selemat et al [69] stated that cubic nitrides could appear in different stages of non-stoichiometry. The X value in TiN_x could be obtained between 0.5 to 1.1, and the X value depended on the percentage of nitrogen in the processing environment [69]. In addition, the X value is close to 1, the Nitrogen content is 100 %, whereas, 80 % of nitrogen content corresponds to an X value of 0.8 [69]. The concentration of TiN_x is inversely proportional to the depth of the nitride layer [35]. Increasing of the depth from surface reduces the amount of TiN_x precipitates. This means that the overall phase transformation on the top surface is not equal to the depth below 300 µm below the surface [70].

For the conventional laser gas nitriding, the volume fraction and distribution of the TiN phases strongly depend on the nitrogen content in the nitriding condition [36]. The very low nitrogen content contributed to the martensitic ά-Ti. When it is over 5 % of nitrogen content in the processing environment, a fine mixture of α- and β-Ti grains appeared due to suppression of martensitic transformation (β-Ti -> ά-Ti) by dissolving nitrogen atom to the solidified body-centred-cubic (bcc) lattice [65, 71]. When it is up to around 11 % of nitrogen content in the processing, a formation of globular and plate-shaped $TiN_{0.3}$ could be observed [65, 71]. Therefore, the structure changed to a mixture of globular and plate-shaped $TiN_{0.3}$ in a metallic fine disperse matrix of α- and β-Ti. With the nitrogen content up to 40 % in the process, δ-TiN dendrites became dominated in the microstructure of laser nitrided Ti-6Al-4V [36]. In addition, the phase of Ti_2N, $TiN_{0.3,}$ α- and β-Ti were discovered in Ti-6Al-4V with hard and brittle nitrides and more ductile metallic components [36]. In the low concentration of nitrogen in the processing, the nitrogen atom dissolved interstitially in the ά- or α-lattice while in the higher concentration of nitrogen, the high amount of nitrogen atom in the melt zone led to the formation of TiN during solidification.

Compared with conventional LGN, the phase transformation of nitrided surface on titanium and its alloys is a more advanced and complicated in diffusion LGN. Several reactions may appear simultaneously at the boundary between atmosphere and material surface. The basic principle of the diffusion nitriding based on Ti was presented by Zhecheva et al. [72]. This simplified model was developed based on reaction of diffusion rules to predict the processing temperature under the β transus temperature. When the titanium material is exposed to the nitrogen atmosphere at high temperature, the nitrogen atom diffuses into the titanium to form interstitial solution of nitrogen in the hexagonal-close-packed (hcp) α-Ti

phase [72]. In the Fig. 3, it shows that the surface layer is called the diffusion zone in terms of α(N)-Ti. This process could be continually repeated irradiating of the same surface until the α or ά-Ti matrix can dissolve more nitrogen atom at the surface of titanium. When the nitrogen concentration on the titanium surface is high, the α phase is not present in interstitial solution, subsequently, the reaction takes place at the interface forming the new Ti_2N phase which is shown in the second row in the Fig. 3. In the same case, when the nitrogen concentration at the interface is further increased, phase transformation occurs at the titanium surface and the Ti_2N transforms to TiN, where Ti_2N is located below TiN. The compound layer consists of TiN and Ti_2N while α- or α(N)-Ti as the diffusion zone is observed underneath the compound layer. This physical model is developed for the diffusion of nitrogen in pure titanium, and it can be deduced by using the reaction diffusion rules to the binary Ti-N phase diagram of the Ti-6Al-4V alloy. Moreover, titanium alloys (e.g. Ti-6Al-4V or NiTi) should be further investigated for confirmation of the actual phase development and stated any differences of microstructure with this basis model.

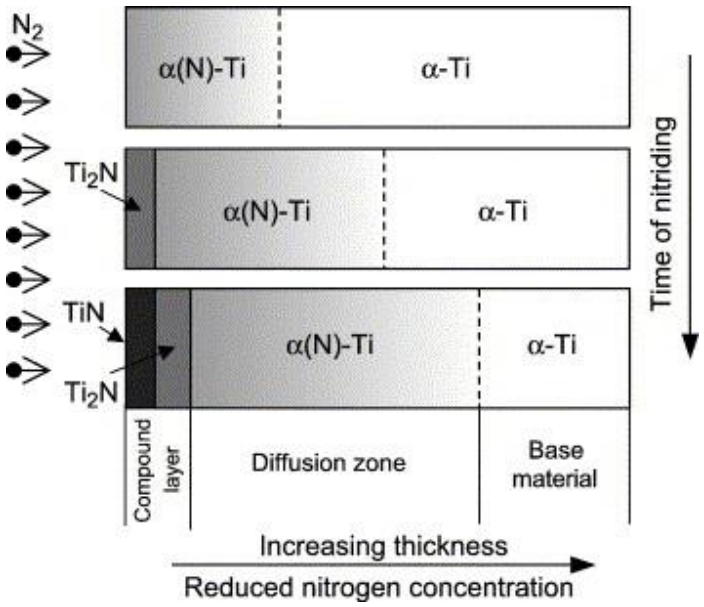

Figure 3 A schematic diagram of the formation and growth of surface layers during diffusion nitriding of titanium [72]

2.5.5. Properties of the Laser Nitrided Surface

2.5.5.1. Surface Roughness

The surface roughness induced by laser nitriding usually depends on the morphologies, such as ridges and periodic structures [70]. From György et al. [73, 74], a rippled structure developed under further laser irradiation might be an effective way to create micro-columns

over the entire nitrided surface. In addition, the nitrogen gas pressure was also a key factor on the surface morphology. When the pressure of nitrogen gas was high, smooth flat islands appeared, accompanied by a wave-like micro-relief plane [74]. An increase in the number of laser pulses, polyhedral structures were also found in the surface plane [74]. Xue et al [71] claimed that surface roughness after laser processing was determined by the laser processing parameters (e.g. nitrogen concentration) and the overlapping ratio between two adjacent laser tracks. Baker [70] also found that the surface roughness of the samples after laser treatment was smoother than that of the as-ground surface and the shot peening surface [68, 71]. Under the 100 % of nitrogen gas environment, both Ti and Ti-6Al-4V alloys could improve the relatively smooth surface to the Ra values of 2.7 µm and 4.6 µm, respectively [68, 71], although these values were still greater than those by laser processing in 100 % argon atmosphere or under a vacuum situation [64].

Therefore, in a word, the nitrogen gas pressure and concentration, laser processing parameters (e.g. laser power), overlapping ratio of two adjacent laser tracks and the number of the laser tracks are the principal determinant factors of surface roughness of nitrided samples.

2.5.5.2. Wear Behaviour of Nitride Layer

A high wear resistance for bio-implant was also concerned as priority. Therefore, surface modification is necessary to increase the surface strength to reduce the wear tendency of titanium and its alloys. Laser nitriding can effectively achieve the surface roughness as micron level so that the wear resistance can be obviously improved [70]. In the findings of Yerramareddy and Bahadur [75], Ti-6Al-4V alloy was tested in both sliding wear and abrasive wear following laser surface treatments, such as surface melting in an argon atmosphere, nitriding and nickel powder deposition where the 25 – 50 µm nickel layer was melted in an argon atmosphere. The results of sliding wear test showed that the steady state wear rate was decreased from 40 x 10^{-4} mm^3 m^{-1} to 0.8 x 10^{-4} mm^3 m^{-1} with nickel powder deposited; a further reduction to 0.5 x 10^{-4} mm^3 m^{-1} was achieved following the surface melting in an argon atmosphere, and the minimum wear rate at 0.3 x 10^{-4} mm^3 m^{-1} was measured in the laser nitrided samples [75]. For the abrasive wear test, the wear rate of the as-received titanium alloys was about 0.16 mm^3 m^{-1}, which was decreased by a factor of 1.5 for the nickel alloying samples and three times lower for the laser nitriding specimen. The higher abrasive wear

resistance of Ti-6Al-4V seemed associated with the improved surface hardness [70, 75]. Moreover, the higher thickness of the TiN layer would cause a greater abrasive wear resistance, even though the fine cracks were still found in the TiN layer [91].

Schaaf et al. [36] studied the pulsed laser nitriding process and compared four time scales of pulsed laser nitriding: the femtosecond, the nanosecond, the microsecond and the millisecond pulsing time scales. It was found the most widespread version was millisecond time scale pulsed nitriding, which the coating fabricated from this process was most satisfied by the typical wear performance and demands [36].

It was also found that sliding wear of laser nitrided samples was dependent on the hard and thick TiN layer with TiN dendrite, which could help abrasive wear improvement even cracks existed. It was recommended to control the nitrogen content during nitriding to avoid unexpected cracks generation [65]. In addition, continuous-wave laser nitriding could be considered improving the wear resistance of metal surfaces [36].

2.5.6. Conventional Laser Gas Nitriding (CLGN)

Laser gas nitriding is one of the categories in laser surface alloying which involves either surface roughening or non-roughening by laser irradiation on the target surface in the nitrogen gas environment. In the conventional laser gas nitriding (CLGN), the surface is roughened in a nitrogen atmosphere to fabricate a nitride layer on the irradiated surface. This nitride layer is metallurgically bonded with substrate and can exhibit superior interfacial adhesion than those produced by other nitriding method, such as plasma and ion implantation [34]. Most of the metallic materials can be nitrided by laser, such as iron, stainless steel, titanium and its alloys. In particular, titanium and its alloys are sensitive to laser processing, the titanium nitride layer can be easily formed under laser irradiation due to higher negative standard Gibbs free energy of TiN formation (-337.7 kJ/mol) [76]. With respect to the various categories and capabilities of the laser, the thickness of the nitride layer can vary from several microns to several hundred microns. Although the CLGN can offer better interfacial properties, two defects that need to be addressed before widespread used, such as roughening surfaces and cracking caused by surface melting [64, 71, 77].

2.5.7. Diffusion Laser Gas Nitriding (DLGN)

In the case of CLGN, the post-treatment is always required after the sample is roughened and cracked, which could take extra cost of materials and experiments as well as time consuming. Man et al [37] hence proposed diffusion laser gas nitriding (DLGN) method to avoid post-treatment process applied. And this method has offered several advantages using in the surface treatment compared to CLGN, such as lower heat energy input & surface temperature, a homogenous coatings fabrication and a disappearance of heat-affected zone. In terms of high quality of solid state diffusion process, a preliminary parameters selection has to be implemented, which allows to narrow down the range of different laser parameters (e.g. laser power, scanning speed, stand-off distance) and minimises the possibility of large heat input. This in turn provides a successful DLGN with the features of non-roughening and uniform surface. Hence, Man et al [37] implemented the preliminary process optimization in the DLGN to avoid significant surface roughening. And the thickness of nitride layer could be increased by repeated laser irradiation on the same track, most importantly, the surface roughness was not affected remarkably after several times of laser irradiation [37]. Compared with CLGN, DLGN also provided consistent high hardness and wear resistance [37].

Previous studies have demonstrated that DLGN could be used to successfully form TiN on Ti alloys (e.g. Ti-6Al-4V) and enhance the wear properties of the alloys. However, Nd:YAG laser was the only laser system applied for laser modification process. The use of other types of lasers (e.g. Fibre laser) has little research on the DLGN. Moreover, their focus was on the mechanical performance and the microstructure characteristics [37]. Therefore, the different titanium alloys (e.g. NiTi) should be further investigated to extend the laser application, and the process optimization with all laser parameters (i.e. laser power, scanning velocity and stand-off distance) should be determined by some well-established systematic methods (e.g. Taguchi Method) to establish standard procedure for industrial application. These considerations have been added as part of this work. If the results are shown to be positive, this approach will become a potential application for practical use.

3. Experimental Details

3.1. Preparation of Metal Substrate

A commercially NiTi-SMA (Ti-50.8 at% Ni) sheet with a thickness of 5 mm was wire electrical discharge machined for the dimensions of 40 mm x 30 mm for laser experiment. The surface of the plates was polished with a series of sand paper until 1200 grits to remove any surface oxides and produce the homogenous surface before diffusion laser gas nitriding (DLGN). The samples were also polished with 1µm diamond paste for 5 minutes, and then ultrasonically cleaned in ethanol bath for 10 mins, rinsed in distilled water, and dried thoroughly in a cold air stream prior to DLGN.

3.2. Process Optimisation by Taguchi Method

Taguchi method is implemented in problem solving and process parameters optimisation [78]. In general, massive various parameters could potentially influence the process of laser gas nitriding, such as laser power, scanning speed, beam diameter, focal distance and nitrogen gas flow rate. In particular, laser power, scanning speed and beam diameter were identified to be most sensitive to impact laser surface treatment to control surface quality [79, 80]. Therefore, a Taguchi orthogonal array design L9 experiment with fixed nitrogen gas flow rate was conducted to investigate the effect of laser parameters to the nitride layer formation with maximum track width in non-melted condition. The width of TiN coverage was acquired using an image processing program ImageJ (downloaded from the NIH website: https://imagej.nih.gov/ij/). Maximisation of the track width and a desirable non-roughened TiN surface are two primary objectives to optimise the laser treated surface, which was chosen for the micro-structural analysis and wear performance. Each set of experiment included 3 control factors while 3 levels were defined in each factor. The factors were specified as laser power, scanning speed and beam diameter. In order to determine the optimal parameters for DLGN, the factors were initially tuned in a predefined range. For instance, the laser power was tested in the range of 80 to 100 W; the scanning speed was varied between 60 and 240 mm/min; the beam diameter was selected from 1.1 to 2.2 mm. The details of parameters applied are listed in Table 1. Three replicates were performed for every set of experimental condition.

Table 1 Levels of each laser parameter

	Level 1	Level 2	Level 3
Power (W)	80 W	90 W	100 W
Scanning Speed (mm/min)	60 mm/min	120 mm/min	240 mm/min
Beam diameter (mm)	1.1 mm	1.6 mm	2.2 mm

Maximisation of the track width via the DLGN process could obtain the non-roughened nitride surface and improve the effectiveness and efficiency of the laser processing. The signal-to-noise ratio (S/N) was determinant to control the responses and reduce the variances, which can be analytically predicted by the constitutive equation below and applied in the present study [81].

Equation 3 S/N ratio equation

$$S/N_L = -10\log(\frac{1}{n}\sum_{i=1}^{n}\frac{1}{y_i^2})$$

where n is the number of replication and y_i can be obtained by the experimentally observed data. Through the application of Taguchi method, the experiment time can be minimised accordingly. In addition, this approach helps to randomise all factor levels to give an equal opportunity for influence from the noise factors. Owing to these two benefits, the effects of the DLGN parameters on the design objective were analysed by MiniTab 17.

3.3. Diffusion Laser Gas Nitriding (DLGN) Procedures

A 100 W CW fiber laser (SP-100C-0013 provided by SPI and A&P Co., Ltd, UK) with output wavelength of 1091 nm was used in the laser nitriding experiment. The samples were processed in a specific gas chamber containing high purity N_2 gas (99.99%). The gas flow rate was controlled at 40 L/min. The samples were processed in a self-constructed chamber and the laser interaction point was continuously shielded with pure nitrogen gas at a rate of 40 L/min. The purpose of using pure nitrogen gas was for oxidation prevention and good condition of Titanium Nitride (TiN) formation by creating stable nitrogen zone. It should be noted that the target material and laser experimental set-up were held in a laser safety cabinet in which the ambient gas was air. Moreover, an extraction system was used to remove any exhausted gas formed during DLGN process.

3.3.1. Selective Area Diffusion Laser Gas Nitriding (DLGN)

In order to control the surface coverage ratio, two different hatch patterns, namely 1 mm (H1) and 3 mm (H3) between the nitride tracks, were designed during the nitriding process. In addition, a wholly nitrided (WN) and polished sample (P) were used. The applied laser scanning patterns were illustrated in Fig. 4. To provide an accurate and quantitative estimation, the surface morphology was firstly captured by optical microscopy (OM, Leica DM4000M, Germany). The captured images were exported as a high resolution micrograph which is shown in Fig. 5a. The total nitrided area was directly measured from the optical micrograph by manually selecting the boundary of nitrided zone and untreated zone using ImageJ (see Fig. 5b). The ImageJ helped to measure the percentage of nitrided area by manually identifying the golden yellow colour. In Fig. 5a, due to the colour contrast between the bare NiTi (silver colour) and TiN (golden yellow colour) capturing under microscopy, the brown colour observed in Fig. 5a was represented by the TiN (golden yellow colour) and the yellow colour (in Fig. 5a) indicated that the bare NiTi exist. The nitrided zone was measured with the red colour indication as shown in Fig. 5b. The yellow colour observed in Fig. 5 was unselected manually which was to avoid the surface area calculation including the bare NiTi area. The total nitrided area was then calculated by the ImageJ in terms of mm^2.

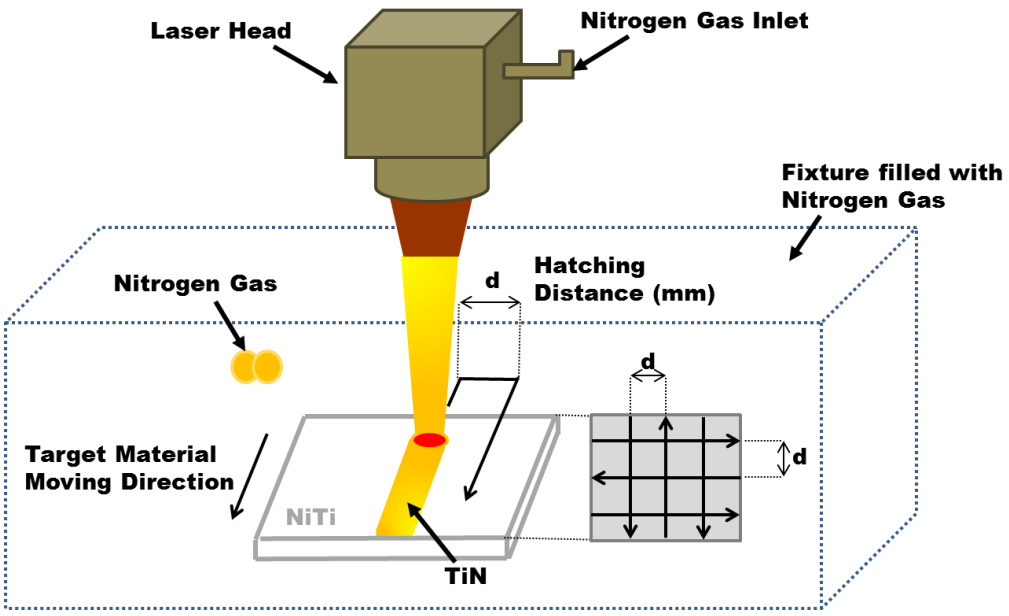

Figure 4 Schematic diagram showing the laser scanning patterns [82]

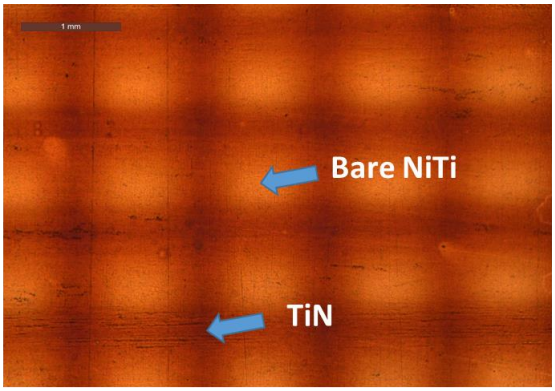

(a) Optical micrograph of the H1 laser induced pattern before ImageJ analysis

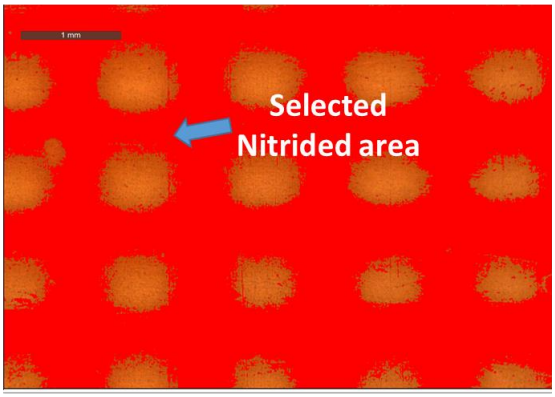

(b) Optical micrograph of the H1 laser induced pattern after ImageJ analysis

Figure 5 Example of showing the ImageJ measurement on the laser nitrided sample [82]

3.4. Microstructural and Surface Characterization

The cross-section of samples was polished by 1µm diamond paste for 5 minutes and the surface was swabbed in the etching reagent (HF 10%, HNO_3 40%, H_2O 50%) for metallographic characterisation by 15 seconds, which was observed by scanning electron microscope (SEM, JEOL Model JSM-6490, USA). An X-ray diffraction (XRD, Bruker D8 Advance, USA) was used for the phase identifications on the surface of nitrided and untreated sample. The parameters were set at 40 kV and 25 mA using Cu Kα radiation with a scanning rate of 1° min^{-1} and various 2θ angles from 20° to 90°.

Morphological analysis, in terms of surface roughness R_a, nitrided and untreated samples were compared by a non-contact surface profilometery (IFM G4 System, Alicona, Austria) with surface map software. The 3D profiler was set up using a 5x resolution probe at a working

distance of 20 mm. The set-up parameters for the 3D profile measurement were defined as follows: size = 3 mm x 4 mm, standard implemented = ISO 4287.

3.5. Wettability Assessment

3.5.1. Static Contact Angle Measurement

The surface hydrophilicity/hydrophobicity of the laser nitrided and bare NiTi were examined by sessile droplet method with the aid of contact angle goniometer OCA 20 DataPhysics and a CCD video camera. The samples were ultrasonically cleaned in an ethanol bath for 5 min and dried thoroughly in a cool air stream between measurements. Distilled water and diiodomethane were used as the reference liquids to acquire the data of surface free energies of each specimen. The volume of each sessile drop was controlled at 2 ± 0.1 µl using a microliter syringe which is small enough to ignore the effects of gravity. Droplet images were captured in the direction perpendicular to the laser track orientation at fixed time intervals, counting since the start of droplet placing on the sample surface to the cessation of droplet spreading (i.e. at least 60 s). The mean value and standard deviation of contact angle value were then calculated from the experimental data of at least 5 repetitive tests on the same sample.

3.5.2. Surface Free Energy Calculation

Owens-Wendt (O-W) (Equation 4) [83, 84] and Neumann equation of state (Equation 5) [85] were used in the current study to determine the surface free energies of the laser nitrided and untreated samples. Surface energy of sample surface was calculated via static contact angle measurements according to the Owens-Wendt (O-W) (also called as Geometric mean approach) and Neumann equation of state, which are based on well-known Young's equation for the calculation [86].

For the Owens-Wendt (O-W) method [83, 84], it followed Fowkes' ideas [87, 88, 89, 90] that the surface free energy comprised two components: London dispersion interaction γ^d and polar (non-dispersive) γ^p component.

Equation 4 Owens-Wendt (O-W) method

$$\gamma_L(1+\cos\theta) = 2\sqrt{\gamma_S^d \gamma_L^d} + 2\sqrt{\gamma_S^P \gamma_L^P}$$

where the dispersion component is referred to γ^d and polar component is represented by γ^p, whereas, γ_S represents the solid surface and γ_L represents liquid surface. The surface tension and energy components of distilled water and diiodomethane are shown in Table 2.

Table 2 Surface tension and its components of the distilled water and diiodomethane at 20°C, in γ mJ/m²

Liquid	γ	γ^d	γ^p
Distilled Water	72.8	21.8	51.0
Diiodomethane	50.8	50.8	0

Solid-liquid interface tension in the equation of state could be obtained by the work of Kwok and Neumann [85]. β (β = 0.0001247 m^2/mJ) in the equation of state is a constant of the interfacial system which was determined experimentally [85]. Combining the Young's equation with the Kwok and Neumann equation, the surface energy can be calculated by the measured contact angle.

Equation 5 Neumann equation of state

$$\gamma_L(1+\cos\theta) = 2\sqrt{\gamma_S\gamma_L}e^{\beta(\gamma_S-\gamma_L)^2}$$

3.6. Wear Resistance Analysis

The coupling of Titanium alloys and Ultra-High-Molecular-Weight Polyethylene (UHMWPE) represents the bearing pair challenged in orthopaedic implants, namely metallic femoral ball head against plastic acetabular [91, 92]. The evaluation of the wear behaviour of laser nitrided and untreated NiTi against UHMWPE is an important criterion to identify the long-term performance of suggested implant material in wear pair for the life of total joint prostheses. Reciprocating wear tests were employed to assess the wear properties of nitrided and untreated NiTi samples against UHMWPE. Linearly reciprocating pin-on-plate sliding test was performed with Hanks' balanced salt solution as a lubricant under the ambient conditions (TE99 Universal Wear Machine, Phoenix Tribology, UK). A schematic diagram of the pin-on-plate machine is shown in Fig. 6. The nitrided and untreated plate were located on a turntable driven at a constant speed of 0.12 m/s and UHMWPE pin was loaded at a contact stress of around 2 MPa by means of static weights. The friction force was recorded by the computer and converted into friction coefficient data. The average specific wear rate of UHMWPE, nitrided and untreated surface were calculated using the Archard equation [56, 57]:

Equation 6 Archard equation

$$Wear\ factor\ (mm^3N^{-1}m^{-1}) = \frac{Volume\ loss\ (mm^3)}{Sliding\ distance\ (m)x\ Load\ (N)}$$

The wear factors for the nitrided and untreated surfaces were obtained, and the average percentage of the weight change was also determined. The results were taken from the average of three repetitive tests with the standard deviation for comparing each type of samples. After the wear tests, the wear tracks which were observed under an optical microscope were compared. All values were expressed as means ± standard errors.

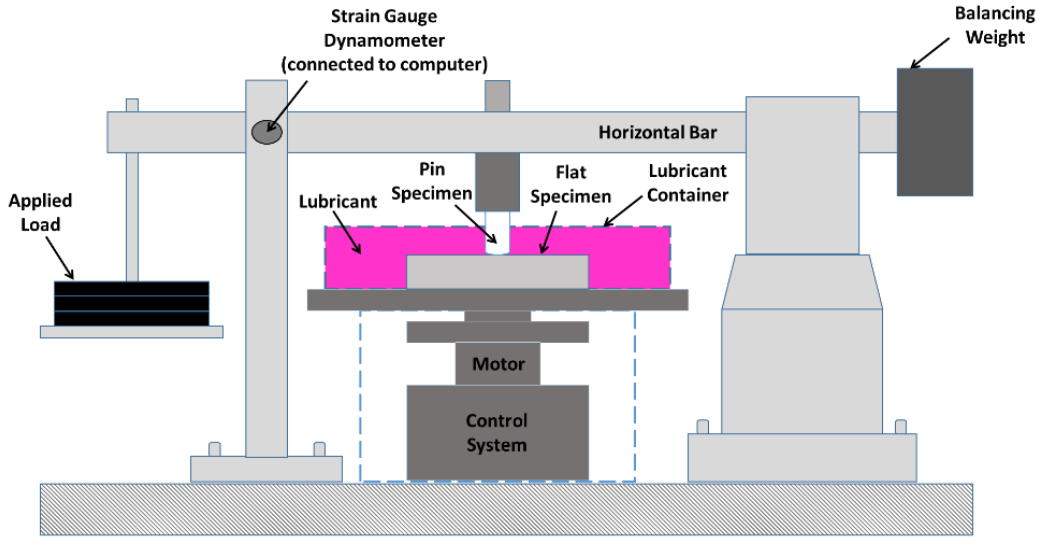

Schematic diagram of pin-on-plate machine

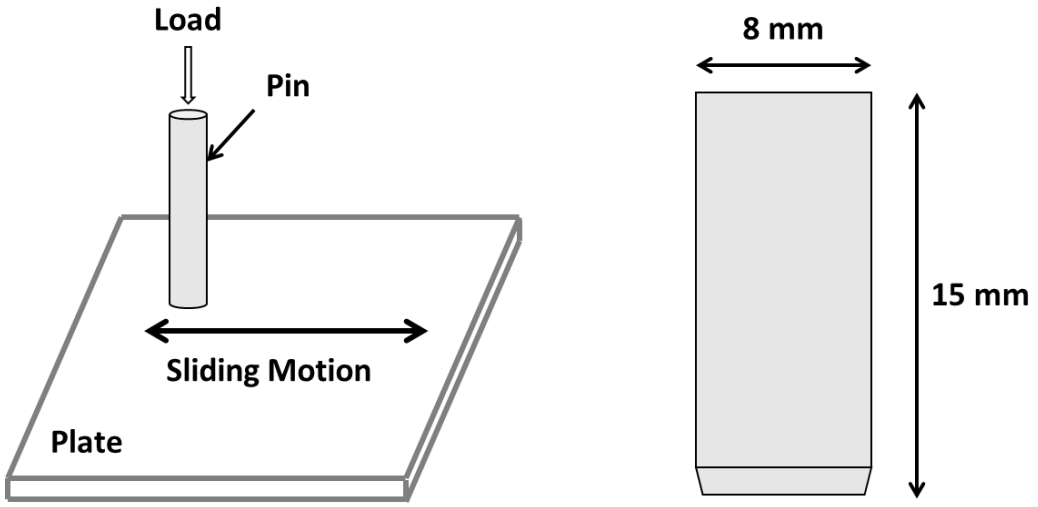

Test Configuration **Truncated Conical End Pin**

Figure 6 Schematics of pin-on-plate tribo-meter, test configuration and test pin [82]

4. Results and Discussions

4.1. Taguchi Analysis

4.1.1. Signal-to-Noise Ratio (S/N ratio)

S/N ratio was analysed by the conceptual approach, which mainly focus on identification of the optimal factors [93]. The S/N ratio assess how individual factors may predict the responses. The signals are an indication of average responses effectiveness, and the noises were derived based on the average responses. In this work, two objectives using Taguchi analysis were of most interest: (1) to acquire the most efficient DLGN on the surface of NiTi; (2) to obtain a desirable non-roughened surface. The maximum width of the laser track was determined to ensure the DLGN successful without surface roughening. In addition, since the goal of the experiment is to maximise response, the larger S/N ratio, the better the outcome. The width of laser track and the calculated S/N ratio for nine experiments are listed in Table 3. The graphical results of different laser parameters with 3 different levels are shown in Fig. 7. The maximum average S/N ratio corresponds the optimal parameter level to the smaller variance of the output characteristics at the desired value. Consequently, highest point in each plot indicated that recommended level for each laser parameter. The results in Fig. 7 suggest that the laser power at level 2 (90 W), the scanning speed at level 1 (1 mm/s) and the beam diameter at level 3 (2.2 mm) to obtain the widest laser track without roughening the surface.

Table 3 Results for the width of TiN coverage and calculated S/N ratio [82]

Run	Power (W)	Scanning Speed (mm/s)	Beam Diameter (mm)	Measured Width of laser track (mm)	Calculated S/N ratio (Larger-the-better)
1	80	1	1.1	1.00	-0.02
2	80	2	1.6	1.23	1.79
3	80	4	2.2	1.14	1.06
4	90	1	1.6	1.94	5.75
5	90	2	2.2	1.42	3.02
6	90	4	1.1	1.24	1.83
7	100	1	2.2	1.79	5.01
8	100	2	1.1	1.13	1.08
9	100	4	1.6	1.03	0.22

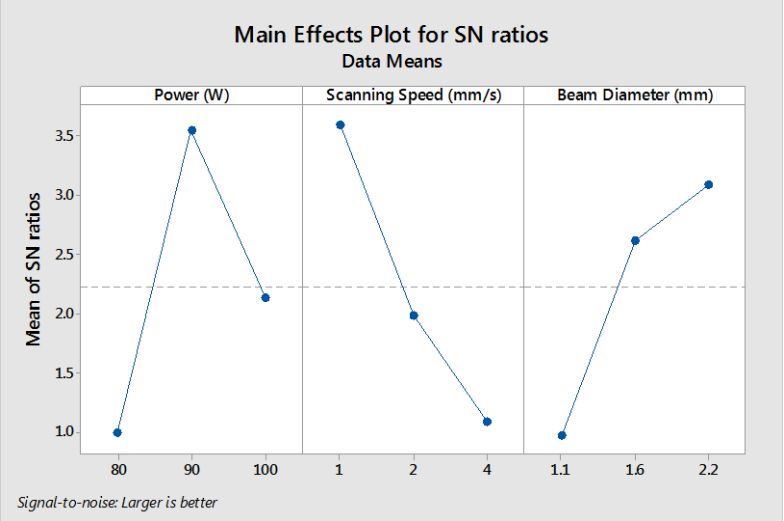

Figure 7 Means of the S/N ratios for each laser parameters [82]

4.1.2. Analysis of Variance (ANOVA)

The results shown in section 4.1.1 could indicate the differential response at different experimental parameters, but it is unknown whether such difference is due to random experimental errors or due to true differences. ANOVA is a useful statistical method to objectively identify differences relative to the internal variability (i.e. random experimental errors). In the ANOVA analysis, a larger F ratio indicates a higher difference relative to the internal variabilities and usually considered significant if the F ratio is larger than 4 [94]. In addition to the F ratio, variation resulting from the individual processing parameter was evaluated by percentage of contribution (P), i.e. the higher the percent contribution, the higher the influence. Table 4 shows the result of ANOVA for different laser parameters. The F

ratio of Power, Scanning Speed and beam diameter were both lower than 4, indicating that the effect of change in the level of the three laser parameters to the diffusion laser gas nitriding process is insignificant. Among three laser parameters, the laser power was the strongest factor to affect the nitriding process by its highest percentage of contribution, which followed by the scanning speed and the beam diameter. The P of the laser power was 30.54% while the scanning speed and the beam diameter accounted for 30.29% and 21.68%, respectively. The P of error was found to be 17.48%. This value, smaller than 50 %, indicates that no important factors were omitted or significant measurement error was involved. Moreover, the Delta statistics in Table 5 were additional way to assess the importance of individual parameters for the response. Delta statistics measured the effectiveness of output characteristic by taking the differences between the highest and lowest average values for the response characteristic [95]. The process parameter was ranked from highest to lowest importance according to the delta values. Consistently, the laser power was the most determinant parameter to measure the effectiveness DLGN; the scanning speed was second and the beam diameter showed the least importance. From the above analysis, the level 2 of laser power (i.e. 90 W), the level 1 of scanning speed (i.e. 1 mm/s) and the level 3 of beam diameter (i.e. 2.2 mm) were selected as the optimised laser processing parameters for producing the wholly nitrided (WN) and all hatch patterns (i.e. H1 & H3) samples for wettability and wear assessment.

Table 4 Analysis of the variance for S/N ratio of different laser parameter [82]

Source	DF	Seq SS	Adj SS	Adj MS	F	Percent Contribution, P
Power (W)	2	10.14	10.14	5.07	1.75	30.54
Scanning Speed (mm/s)	2	10.05	10.05	5.03	1.73	30.29
Beam Diameter (mm)	2	7.20	7.20	3.60	1.24	21.68
Residual Error	2	5.80	5.80	2.90		17.48
Total	8	33.19				

Table 5 Response table for S/N ratio of different laser parameter [82]

Level	Power (W)	Scanning Speed (mm/s)	Beam Diameter (mm)
1	0.94	3.60*	0.96
2	3.54*	1.96	2.59
3	2.12	1.04	3.05*
Delta	2.60	2.56	2.08
Rank	1	2	3

Total mean of S/N ratio = 2.20; *Optimized level of parameters

4.2. Microstructural and Surface Analysis

4.2.1. Microstructural Analysis

Ni ion release from NiTi has two main sources [96]: the Ni-containing surface of the oxide layer which was responsible for the short term Ni release (≤ 21 days), and the Ni-rich layer underneath the oxide responsible for the long term Ni release (8 months). Increasing the content of the Ni ions within the surrounding tissue would generate inhibition on pathways associated with actin cytoskeleton[1], focal adhesion[2], energy metabolism[3], inflammation[4] and amino acid metabolism[5] [97]. Therefore, the TiN coating was purposed to improve endothelial cell function, increase energy metabolism, enhance regulation of inflammation and promote amino acid metabolism by the effective prevention of Ni ions release from NiTi [97]. Moreover, Ni ion released from NiTi implant reduced significantly when the TiN coating is fabricated by the laser gas nitriding (LGN) method [77]. In this study, Ni-depleted surface arising from the TiN coating by DLGN was developed to enhance biocompatibility of NiTi where this surface could assist the inhibition of short term and long-term Ni ion release.

The laser nitrided sample was carried out by the optimal parameter combined with fixed nitrogen gas flow rate. A golden colour was observed on the sample surface, indicating the formation of TiN. The SEM image of the cross-sectional TiN layer is shown in Fig. 8. It can be clearly seen that the uniform TiN layer of approximate 2 µm was formed. The DLGN method seemed to be the most ideal to provide coating with consistent thickness and better surface finish. It also has no heat affected zones, i.e. any cracking or porosities and reduced part distortion. The binding energy of the crystal lattice and the diffusion rate of Ni ions through the barrier layer were two of the most predominant factors to affect the Ni ion release rate from NiTi substrate to the surrounding tissue where the thickness of the coating on the surface of NiTi was inversely proportional to the Ni ion release rate [98]. In addition, cracking is a major concern in the laser nitriding process, especially in thick layer formation because

[1] The cytoskeletion mainly composes of actin filaments and microtubules that offer a suitable mechanical support and plays an important role in cell shape, differentiation and movement.
[2] Focal adhesion is a type of adhesive contact to serve as mechanical linkages to the extracellular matrix and cells.
[3] It is the process of using nutrients to the energy (ATP) generation, and composes a wide variety of interconnected pathways that can work in whether the presence of oxygen or not.
[4] It is related to an infection, injury or illness to give rise to painful redness of the human body.
[5] It is the process to transfer the protein food inside the body to make tissue proteins, and these proteins are used to produce energy after a break down process.

the formation of large and brittle titanium nitrides strongly promoted cracks, minimising the effectiveness of TiN coating. A micron level thick TiN coatings could accommodate more than 1% elastic strain without cracking [99], hence, the current method to create high performance TiN coating (around 2 µm thick) on the NiTi to inhibit Ni ion release is possible. This method was expected to improve biocompatibility of NiTi implant even the uniform TiN layer was about 2 µm thick. There is also an explanation of DLGN method that can suppress the release of Ni ions from NiTi substrate. In this method, nitrogen (N) is firstly absorbed at the surface under laser irradiation which is then diffused inward into NiTi at elevated temperatures. Rapid diffusion of N into the surface of NiTi during laser processing will first form an interstitial solution in NiTi. Upon saturation of this interstitial solution, TiN will eventually be formed on the surface due to the great affinity of Ti for N [91]. When TiN is formed on the surface by consuming Ti from NiTi substrate, a Ni-rich phase will be depleted from the surface and formed in the substrate due to the conservation of matter. Therefore, the depletion of Ni in the surface layer after nitriding is expected.

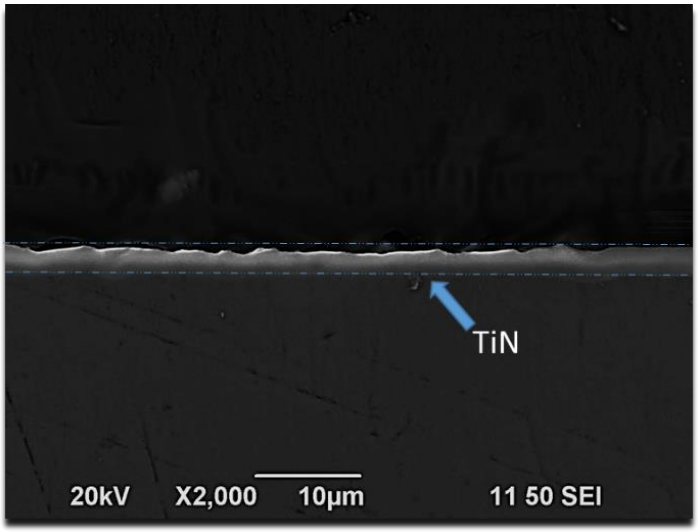

Figure 8 SEM micrograph showing the cross-section view of TiN layer [82].

4.2.2. Phase Characterisation

The XRD patterns of the optimised laser nitrided and untreated surface are shown in Fig. 9. On the untreated surface, no additional diffraction peaks were observed, which correspond to intermediate precipitations, namely Ni_3Ti and Ni_4Ti_3. The untreated NiTi only consisted of the NiTi (B2) phase, which is also known as the austenite phase. The major component of the untreated NiTi was austenite at room temperature. As observed from Fig. 9, the laser nitrided

NiTi had two distinct peaks, corresponded to cubic titanium nitride (TiN) preferentially grown on (200) and (311) plane. The intensity of the TiN (200) peak was much stronger than that of the TiN (311) peak. There were no other peaks detected from the laser nitrided NiTi surface and the intensity of diffraction peaks of NiTi (B2) phase was suppressed, indicating that the pure TiN layer was formed on the NiTi surface. Moreover, the laser gas nitriding process did not affect the phase composition of NiTi substrate due to absence of intermediate precipitation of XRD patterns.

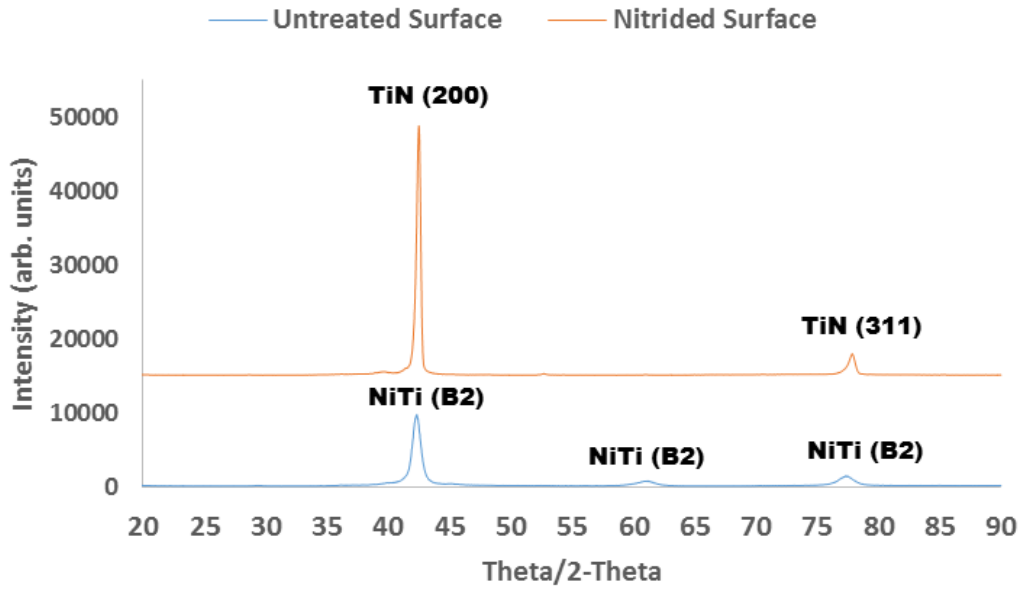

Figure 9 XRD patterns of the laser nitrided and untreated surface [82]

4.2.3. Surface Roughness Analysis

Surface characteristics of NiTi are critical to evaluate the performance of the implant on tissue responses. It is also crucial to understand its material reaction to physiological environment due to a direct contact between the implant material (e.g. NiTi) and the surrounding tissue. For the laser irradiation on the samples' surface, the surfaces would rise in temperature and be melted when the threshold of melting of the laser-material interaction was reached. Scanning a predetermined pattern across the NiTi surface gave rise to a significant variation in surface topography and roughness when compared with the untreated samples. In this analysis, the nitride surface (i.e. WN, H1 & H3) and the polished surface showed similar surface features and 3-D morphology under the 3-D profiler measurement. The nitride surface became less apparent compared with the polished sample via the 3-D image observation, and the typical 3-D profiles image is shown in Fig. 10. It can be deduced

that the optimised DLGN process gave low temperature and energy input to the sample surface, and the wholly nitrided (WN) samples exhibited similar surface features to polished samples, in terms of the highest maximum peak heights Table 6. It was found that the patterned samples (H1 and H3) had larger surface roughness values in comparison with the polished sample and WN sample, which was attributed to the hatch patterns. These patterns had discrete TiN coating and untreated surface on the sample, and a single pass of the laser beam induced a periodic pattern, causing a slight increase in surface roughness. For the case of WN sample, the more the surface area was irradiated by laser, the more homogenous TiN layers were formed. Thus, the periodic pattern would not exist and the whole surface was covered by homogenous TiN layer. As a result, the surface roughness R_a of the WN sample slightly increased where the maximum peaks' heights increased to 1.30 ± 0.21 µm (Table 6).

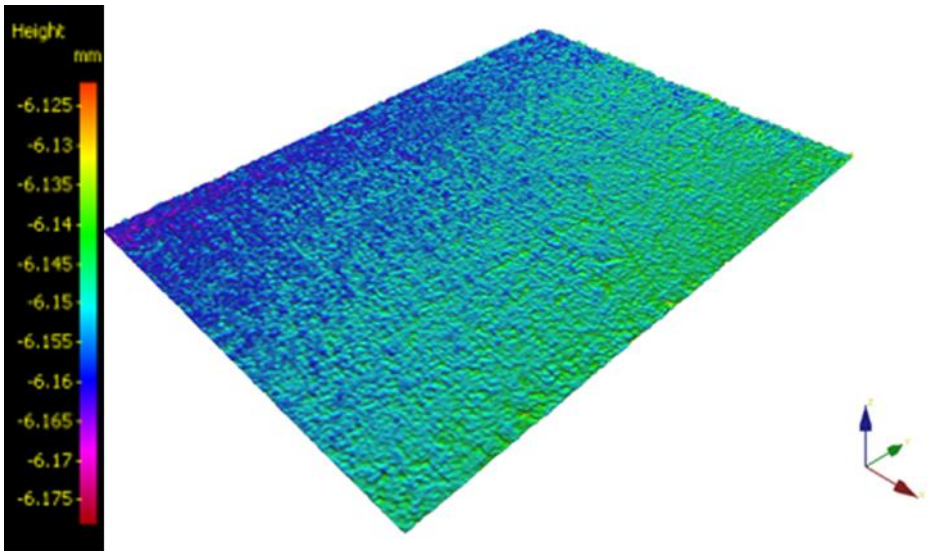

Figure 10 A typical 3-D profiles image for polished, WN, H1 and H3 samples.

Table 6 The surface roughness, area coverage of nitrided and untreated area across target material [82]

Sample	R_a (nm)	R_p (µm)	Nitrided Area coverage	Untreated Area Coverage
WN	277.23 ± 28.60	1.30 ± 0.21	100%	0%
H1	324.59 ± 23.27	2.29 ± 0.95	76%	24%
H3	322.23 ± 45.74	1.99 ± 0.99	52%	48%
Polished	248.03 ± 26.09	1.15 ± 0.17	0%	100%

4.3. Wettability Study

To investigate the wetting properties of the treated surface, the contact angle was measured using distilled water and diiodomethane. The results of probe liquid (degree) and

their standard deviations are given in Table 7. The mean value was obtained from 5 contact angle measurements on the droplets of given probe liquid settled on the specimen. According to the American Society for Testing and Materials D7334-08 specifications [100], when the water contact angle is less than 45°, the surface is hydrophilic; when the contact angle exceeds 90° the surface is hydrophobic. The NiTi surface shows a hydrophilic tendency after laser treatment. The lower contact angles of distilled water and diiodomethane were found in laser nitrided sample, which indicated that the surface hydrophobicity of NiTi was reduced after DLGN. Furthermore, the decrease in the contact angle of distilled water was more profound than those of diiodomethane for the nitrided NiTi, possibly because of more polar components on the surface of nitride NiTi that attracts strongly to water molecules (distilled water is polar liquid). Since diiodomethane was a nonpolar liquid, minor change was expected due to the absence of polar interaction between the diiodomethane molecules and the nitride surface.

*Table 7 Average contact angle of probe liquids (°) and their standard deviations measured on the bare and nitrided NiTi samples surface. * P value is smaller than 0.05 was considered as significant difference.*

Liquids / Sample	Distilled Water (°)	Diiodomethane (°)
Bare NiTi	74.78 ± 1.58	49.83 ± 1.05
Nitrided NiTi	68.13 ± 2.20 *	47.05 ± 0.64 *

Results of total surface free energy measurements for nitrided and bare NiTi are shown in Table 8. It can be clearly seen that the laser treated sample has higher surface free energy than bare NiTi. The values of polar and dispersive components obtained from O-W method are illustrated in Table 9. It shows that a higher surface free energy was measured for samples treated by laser nitriding. In addition, the nitrided NiTi became more hydrophilic with lower values of contact angle and higher value of the polar component. This finding was consistent with the literature [101]. It was also found that a hydrophilic-hydrophobic coupling can facilitate the efficiency of lubrication due to the presence of pressed water film between the tribo-pair. Low wear rate and low friction coefficient are the evident to support hydrophilic-hydrophobic coupling in the tribological system (see Fig. 11 and 12). UHMWPE is hydrophobic, and the nitrided NiTi is more hydrophilic than bare NiTi, so they would improve lubricating effect and reduce friction and wear between the tribo-pair.

*Table 8 Total surface free energy (mJ/m²) of bare and nitrided NiTi samples surface calculated from Owens & Wendt (O-W) and Neumann equation of state. * P value is smaller than 0.05 was considered as significant difference.*

Surface Free Energy / Sample	Owens & Wendt Method (mJ/m²)	Equation of State Approach (mJ/m²)
Bare NiTi	41.15 ± 1.11	38.74 ± 0.98
Nitrided NiTi	45.39 ± 1.33 *	42.86 ± 1.36 *

*Table 9 Dispersive and polar components (mJ/m²) of surface free energy of bare and nitrided NiTi samples from Owens & Wendt (O-W) calculation. * P value is smaller than 0.05 was considered as significant difference.*

Sample	Dispersive Components (mJ/m²)	Polar Components (mJ/m²)
Bare NiTi	34.37 ± 0.59	6.78 ± 0.54
Nitrided NiTi	35.90 ± 0.35 *	9.49 ± 1.00 *

4.4. Wear Behaviour

Wear resistance of the NiTi articulating implants is a crucial factor for its whole service life in hard tissue replacement. A massive amount of microscopic particles could be produced in the movement of artificial joints which are worn off during motions. Titanium nitrides is an ideal choice for wear resistant materials because the nitride layer fabricated on the Ti alloys' surface could reduce cracking and avoid the rapid failure during the movement of artificial joints.

Coefficient of friction (COF), defined as friction over load applied, was recorded between the contact of the pin (i.e. UHMWPE) and the plate (i.e. NiTi or nitrided NiTi) across the entire experiment. Fig. 11 depicted the COF of nitrided and polished samples. For most nitrided NiTi, the COF signals were fairly stable without remarkable changes over the entire sliding distance, except for first few sliding cycles. The COF of polished NiTi was relatively less stable compared with laser nitrided samples. COF was quickly increased to 0.14 within the first few sliding cycles, gradually reached the top (0.26), and finally maintained the value of 0.24, because of more severe wear of the pin (i.e. UHMWPE) and plate (i.e. polished NiTi). In the comparison with the COF of polished sample, both nitrided samples (i.e. WN, H1 and H3 samples) increased slightly after several number of sliding cycles and were finally kept between 0.02 and 0.04. The low values of friction coefficient are typical phenomenon for TiN coatings sliding against UHMWPE [102]. Severe worn off was not shown on nitrided samples due to the

consistently low level of friction coefficient (i.e. between 0.02 and 0.04) across the entire sliding distance. In addition, improved water lubrication leads to the reduced friction and wear of the tribological interface, i.e. the metallic surface and UHMWPE. As reported in chapter 4.3, improved water wettability of the laser-treated NiTi samples (static water contact angle from 74.78° to 68.13°) can support the hypothesis that the TiN formation on the NiTi surface and led to reduced friction and wear factor of the tribo-pair. Therefore, the wear resistance of nitrided NiTi was better than that of polished NiTi with the lower COF and wear factor (see Fig. 11 and 12).

A higher wear factor indicates more serious wear damage and hence lowers wear resistance. Fig. 12 shows the wear factor of UHMWPE pins, laser nitrided and polished NiTi surfaces. The wear factors of nitrided samples are lower for overall tribo-system, and the downward pattern is noticeably observed in UHMWPE. The wear factor was decreased by 43.51 % (H3 sample), 87.43 % (H1 sample) and 98.17 % (WN sample) on average after laser nitriding on NiTi surface (see discrete error bars in Fig. 12), confirming the excellent wear-resistant effects of laser nitriding on NiTi surface. Between polished NiTi/UHMWPE and wholly nitrided NiTi/UHMWPE pairs, about 10 times higher wear factor from polished NiTi/UHMWPE pairs can be correlated to its higher COF (see Fig. 11). TiN is much higher in hardness than NiTi and has a higher wear resistance. All these differences were all statistically significant with p-values < 0.05, indicating that the differences were highly unlikely to be due to random experimental errors. The above experimental results indicate that the nitrided NiTi/UHMWPE pair exhibits much better wear behaviour than that consisting of untreated NiTi/UHMWPE pair. Thus enhancing the TiN coverage area favours wear performance. Moreover, the small error bars in Fig. 12 indicate that the wear test results are accepted as reliable, and both nitrided samples demonstrated smaller variations in the wear factors of UHMWPE pins and metal plates. These results ensured that laser nitriding could produce more stable and reproducible wear resistant NiTi samples.

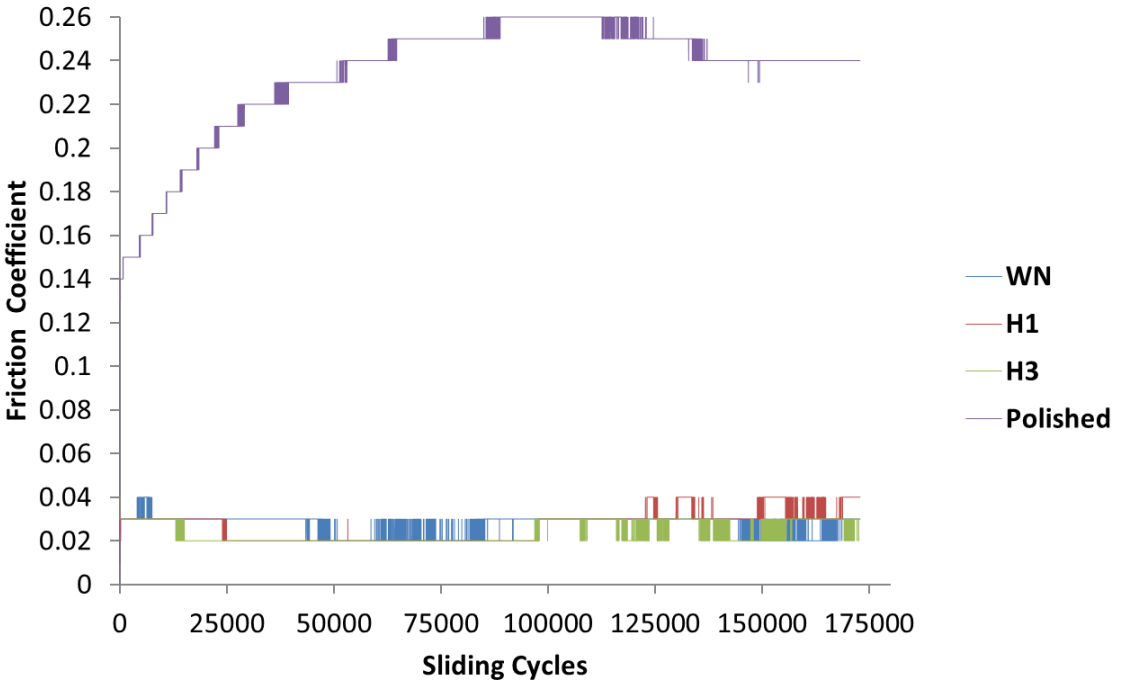

Figure 11 Frictional curves of polished, WN, H1 and H3 samples [82]

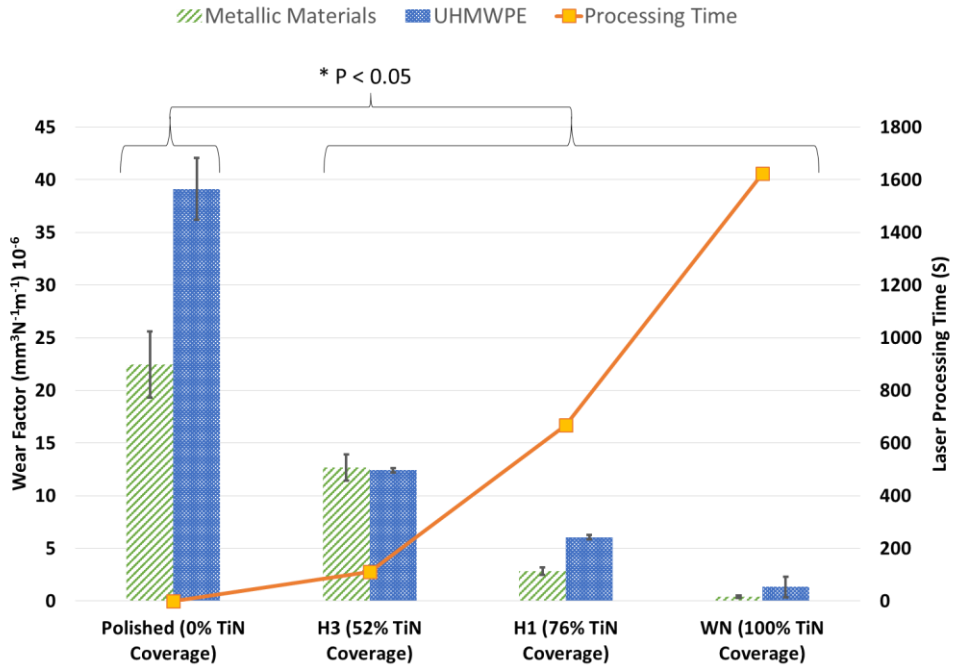

*Figure 12 Wear factor for each samples in relation to laser processing time. * P value is smaller than 0.05 was considered as significant difference. [82]*

Optical morphology of the polished and wholly nitrided surfaces after the wear test are shown in Fig. 13. It can be observed that the sliding tracks are clearly visible from both the polished and the wholly nitrided NiTi. The polished sample showed the formation of several craters on the surface with severe worn off under the same wear condition. The wholly

nitrided sample only presented few shallow sliding tracks, in particular, cracks, flakes and fragmentation were absent. This is in agreement with improvement of wear properties of NiTi by laser treatment due to the formation of hard TiN surface layer. In addition, the higher wear rate of the polished NiTi (smoothest sample, see Table 6) could be explained in the following approach. The same condition with same amount of energy is dissipated in the wear test, the large amount of the energy is used for asperity deformation and laser induced patterning ridges deformation on the rougher samples (i.e. H1 and H3 samples), whilst almost all energy is used for the grooves and craters formation on the polished sample surface.

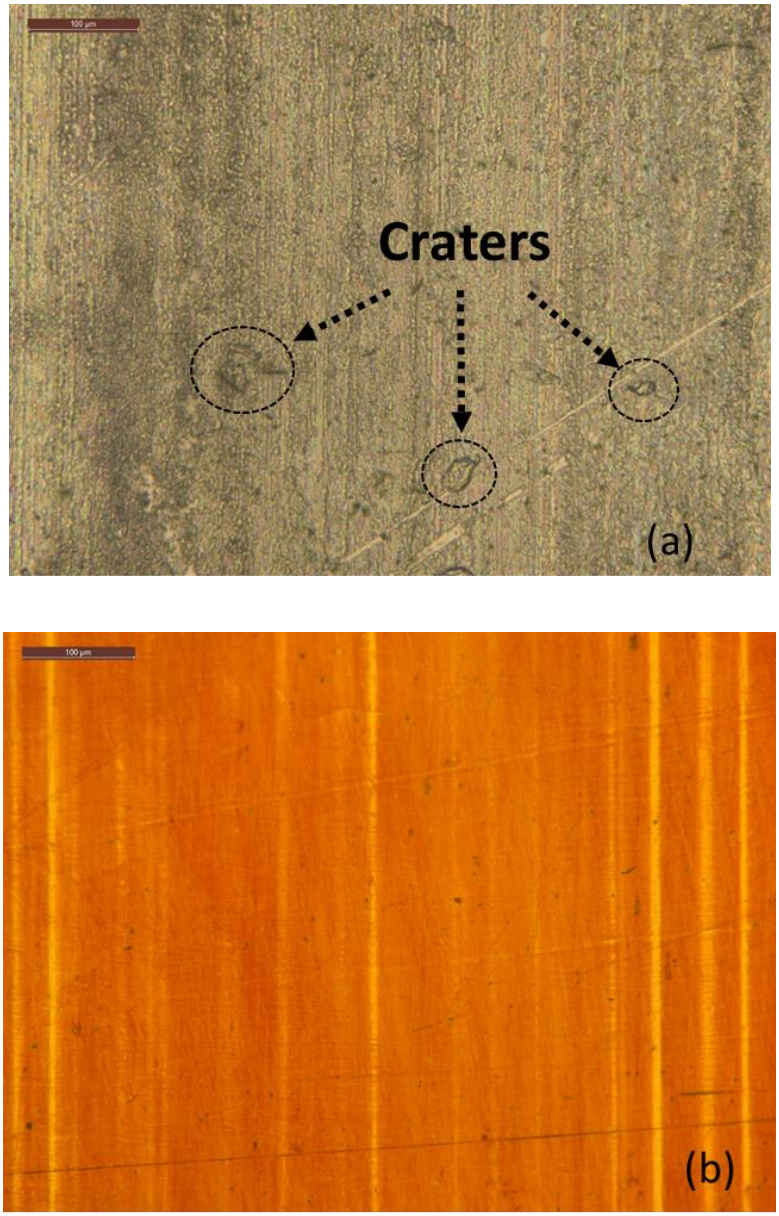

Figure 13 Optical images of the surface of (a) polished and (b) WN sample after wear test [82]

The downward trend was clearer for UHMWPE pins than nitrided NiTi plates, and the reduction of the wear factors was clearly observed (i.e. 68.26 % (H3 sample), 84.51 % (H1 sample) and 96.61 % (WN sample)) which was good evidence for the laser nitriding to enhance wear behaviour of tribo-pair. The improved wear rate of UHMWPE is due to surface wear resistant improvement of the counterpart, namely NiTi by the laser nitriding, especially if three body abrasive wear was the determinant wear mode: Since NiTi is harder than UHMWPE, wear of NiTi surface occurs mainly by NiTi particles as a third body, even though some protruded asperities on the NiTi surface can be initially removed by the UHMWPE surface. Furthermore, the wear factors of UHMWPE were higher than those of the NiTi for both polished and laser treated samples (see in Fig 12). In view of the abrasive wear mechanisms, the hardness of NiTi and TiN were substantially higher than that of UHMWPE, and abrasive wear was expected to occur mainly on the softer side of the tribo-pair, i.e. UHMWPE in this study. Therefore, UHMWPE wear debris could be easily worn off by the harder metal side. Due to the low contact pressure applied in this work, i.e. approximate 2 MPa, adhesive wear was not considered as a major wear mode. Although the Hanks' solution (Cl- ion contained) was used as a lubricant in the wear test and it might induce pitting attack to the metal surface, no pitting was observed from both polished and nitrided surface after wear test. There were no signs of corrosive wear. In this study, it is assumed that the abrasive wear mainly occurred between the tribo-pair. The reason of the reduction was attributed in the wear resistant properties improvement on the counter surface by the formation of TiN. Although the wear mechanism might be different for each case, the common reasons of the wear resistant improvement are the formation of hard coating layer on the target surface and the improved wettability of the target materials.

In summary, the TiN layer formed by laser is attributable for the wear resistant improvement of the tribo-pair. DLGN suggested that there was a correlation between the promotion of wear resistance and the percentage of TiN coverage (see Fig. 12). A longer laser processing time could result in a higher percentage coverage of TiN, thereby increasing the wear resistance of NiTi. However, considering the cost and time required for manufacturing, the partially nitrided surface might be a promising choice that could balance the benefit between manufacturing efficiency and the wear resistance improvement. The H1 sample with 76% TiN coverage is potential candidate for the ball joint in artificial joint, as 59% of laser

processing time could be saved compared with that of the wholly nitrided sample (WN sample). Moreover, over 80 % reduction rate was achieved in the H1 sample for both tribo-pair surface. Therefore, this study helped to recommend the partially nitriding for the field of orthopaedic applications.

5. Summary of Current Study

Owing to the attractive properties of NiTi shape memory alloy, such as shape memory effect, pseudo-elasticity and formability as well as stability, it is a favourable material for the medical components and devices. The Ni content in NiTi shape memory alloy is always the main concern for its long-term performance because the Ni may cause allergy due to the leakage of Ni ions from NiTi substrate. Therefore, conventional laser gas nitriding (CLGN) was proposed to fabricate a TiN film on the NiTi surface, which it not only can prevent the Ni ions from leakage, but also improve the wear resistance so that the debris generation can be minimized during wear between tribo-pair.

It is well known that CLGN can induce a roughen surface due to surface melting occurrence during the nitriding process. Therefore, diffusion laser gas nitriding (DLGN) was purposed to fabricate TiN layer on the NiTi substrate without surface melting and roughening via careful processing parameters selection in this study. The insignificant change of the surface roughness after DLGN is the advantage for the surface modification of NiTi shape memory alloy while it can reduce the need of post-manufacturing.

Taguchi method was applied to investigate the effectiveness of the laser processing parameters on the DLGN with minimised trial experiments where the outcome was used to fabricate TiN on the NiTi substrate. The nitrided surface was compared with bare NiTi by the surface characterization and application performance. Moreover, the wear behaviour of various TiN surface coverage under lubrication condition was investigated. The following conclusions could be drawn:

1. The optimal parameters to form a uniform and non-roughen TiN layer on NiTi surface were found based on Taguchi method: 40 L/min of the nitrogen gas flow rate, 90 W of the optimal laser power is found to be, 1 mm/s of the laser scanning speed and 2.2 mm of the beam diameter, respectively.
2. The surface morphology of bare and nitrided NiTi insignificantly differed, which was determined by optical profilometry. The polar component was increased by DLGN with the TiN formation, although the nonpolar component had enhanced a little bit after the nitriding.

3. A fibre laser could create different percentage of TiN coverage as well as small changes of surface roughness of up to 325 nm and to improve wear factor using a simple but effective hatch pattern.
4. The partially nitrided sample with 76% TiN coverage was a promising solution for improvement of the wear resistance for the artificial joint due to 59% of laser processing time was saved comparing with the manufacturing time of wholly nitrided method.

As the growing demand for a higher quality of life, the need for new technologies has been increasing. These new technologies can be a benefit on pharmaceutical scale and the demand of replacement and revision surgeries. Owing to the ease of automation, chemical cleanliness and fast manufacturing cycle of laser technology, DLGN is a promising method for modifying NiTi articulating implant as well as improving the tribological properties of tirbo-pair. DLGN can also help to propose NiTi as femoral head in artificial hip joint.

6. Suggestions for Future Work

The present study explored laser technology as a feasible tool for improving the surface properties of NiTi, namely hydrophilicity and wear resistance. These results verified that the nitrided NiTi can be an ideal candidate as a tribological safe implant material. Further studies based on the current investigation are suggested taking on this thesis forward.

1. The corrosion is often occurred inside human body as the body fluid is acidic. So using simulated body fluid such as Hanks' solution and Ringer solution for corrosion behaviour analysis is necessary. Therefore, the measurement result may serve as a reference to understand the biomaterials working within body fluid environment.
2. The surface composition should be investigated deeply by TEM, XPS and EBSD in order to make a clear picture of the formation and growth of surface layers during diffusion nitriding of NiTi, and what exact phases are created during the process.
3. As the material is suggested to insert into the human body, the in vitro analysis should be included to evaluate the short- and long-term biological performance. And the cellular mechanisms and biological responses for the nitrided NiTi should be further investigated.
4. The surface Ni content should be analysed by XPS in order to confirm that the Ni content can be reduced by diffusion laser gas nitriding. Moreover, the relationship between the cell responses and Ni content on the nitride surface should be studied. The critical threshold value for Ni content in the nitride surface should be obtained.
5. Animal tests can be involved to examine the bioactivity and biocompatibility of nitrided NiTi in vivo. It is because the information is very useful for clinical application from in vivo experiments.

References

[1] M. Sood, “The challenge of revision hip replacement surgery,” 11 January 2013. [Online]. Available: http://www.arthritisresearchuk.org/arthritis-information/arthritis-today-magazine/159-winter-2013/the-challenge-of-revision-hip-replacement-surgery.aspx.

[2] S. Kurtz, K. Ong, E. Lau, F. Mowat, M. Halpem, “Projections of primary and revision hip and knee arthroplasty in the United States from 2005 to 2030,” *The Journal of Bone & Joint Surgery,* vol. 89, no. 4, pp. 780-785, 2007.

[3] V.M. Goldberg, M.P. Figgie, H.E. 3rd Figgie, M. Sobel, “The results of revision total knee arthroplasty,” *Clinical Orthopaedics & Related Research,* vol. 226, pp. 86-92, 1988.

[4] M. Long, H.J. Rack, “Titanium alloys in total joint replacement -- a materials science perspective,” *Biomaterials,* vol. 19, no. 18, pp. 1621-1639, 1998.

[5] N. Joshi, A. Navarro-Quilis, “Is there a place for rotating-hinge arthroplasty in knee revision surgery for aseptic loosening?,” *The Journal of Arthroplastry,* pp. 1204-1211, 2008.

[6] S.D. Ulrich, T.M. Seyler, D. Bennett, R.E. Delanois, K.J. Saleh, I. Thongtrangan, M. kuskowski, E.Y. Cheng, P.F. Sharkey, J. Parvizi, J.B. Stiehl, M.A. Mont, “Total hip arthroplasties: What are the reasons for revision?,” *international Orthopaedics,* pp. 597-604, 2008.

[7] R.J. Friedman, P. Hirst, K. Kelley, C.B. Sledge, “Results of revision total knee arthroplasty performed for aseptic loosening,” *Clinical Orthopaedics and Related Research ,* vol. 255, pp. 235-241, 1990.

[8] R.P. Katz, J.J. Callaghan, P.M. Sullivan, R.C. Johnston, “Long-term results of revision total hip arthroplasty with improved cementing technique,” *The Journal of Bone and Joint Surgery,* Vols. 79-B, pp. 322-326, 1997.

[9] D.M.T. Brunette, P. Textor, M. Thomsen, Titanium in medicine: material science, surface science, engineering, biological responses and medical applications, Berlin: Germany: Springer, 2001.

[10] F. Kasano, T. Morimitsu, “Utilization of nickel-titanium shape memory alloy for stapes prosthesis,” *Auris Nasus Larynx,* vol. 24, no. 2, pp. 137-142, 1997.

[11] S.A. Shabalovskaya, “ On the nature of the biocompatibility and on medical applications of NiTi shape memory and superelastic alloy,” *Biomedical materials and Engineering,* vol. 6, no. 4, pp. 267-289, 1996.

[12] M.R. Prince, E.W. Salzman, F.J. Schoen, A.M. Palestrant, M. Simon, “Palestrant AM, Simon M. , Local intravascular effects of the nitinol wire blood clot filter,” *Investigative Radiology,* vol. 23, no. 4, pp. 294-300, 1988.

[13] L.S. Castleman, S.M. Motzkin, F.P. Alicandri, V.L. Bonawit, A.A. Johnson, “Biocompatibility of nitinol alloy as an implant material,” *Journal of Biomedical Materials Research,* vol. 10, no. 5, pp. 695-731, 1976.

[14] J. Ryhanen, M. Kallioinen, W. Serlo, P. Peramaki, J. Junila, P. Sandvik, E. Niemela, J. Tuukkanen, “Bone healing and mineralization, implant corrosion, and trace metals

after nickel-titanium shape memory metal intramedullary fixation," *Journal of Biomedical Materials Research,* vol. 47, no. 4, pp. 472-480, 1999.

[15] M.I.Z. Ridzwan, S. Shuib, A.Y. Hassan, A.A. Shokri, M.N.M. Ibrahim, "Problem of stress shielding and improvement to the hip implant designs: a review," *Journal of Medical Sciences,* vol. 7, no. 3, pp. 460-467, 2007.

[16] I. Mihalcz, "Fundamental characteristics and design method for nickel-titanium shape memory alloy," *Periodica Polytechnica Mechanical Engineering,* vol. 45, no. 1, pp. 75-86, 2001.

[17] T. Duerig, A. Pelton, D. Stockel, "An overview of nitinol medical applications," *Materials Science and Engineering A,* Vols. 273-275, pp. 149-160, 1999.

[18] L. Ponsonnet, V. Comte, A. Othmane, C. Lagneau, M. Charbonnier, M. Lissac, N. Jaffrezic, "Effect of surface topography and chemistry on adhesion, orientation and growth of fibroblasts on nickel–titanium substrates," *Materials Science and Engineering: C,* vol. 21, no. 1-2, pp. 157-165, 2002.

[19] M. Bahraminasab, A. Jahan, "Material selection for femoral component of total knee replacement using comprehensive VIKOR," *Materials and Design,* vol. 32, pp. 4471-4477, 2011.

[20] X. Liu, P.K. Chu, C. Ding, "Surface modification of titanium, titanium alloys, and related materials for biomedical applications," *Reports: A Review journal,* vol. 47, pp. 49-121, 2004.

[21] E. Denkhaus, K. Salnikow, "Nickel essentiality, toxicity, and carcinogenicity," *Critical Reviews in Oncology/Hematology,* vol. 42, no. 1, pp. 35-56, 2002.

[22] K. Matsumoto, N.Tajima, S. Kuwahara, "Correction of scoliosis with shape-memory alloy," *Nippon Seikeigeka Gakkai Zasshi,* vol. 67, pp. 267-274, 1993.

[23] P. Rocher, L. El Medawar, J-C Hornez, M. Traisnel, J. Breme, H.F. Hildebrand, "Biocorrosion and cytocompatibility assessment of NiTi shape memory alloys," *Scripta Materialia,* vol. 50, pp. 255-260, 2004.

[24] M.A. Khan, R.L. Williams, D.F. Williams, "Conjoint corrosion and wear in titanium alloys," *Biomaterials,* vol. 20, no. 8, pp. 765-772, 1999.

[25] J. Lincks, B.D. Boyan, C.R. Blanchard, C.H. Lohmann, Y. Liu, D.L. Cochran, D.D. Dean, Z. Schwartz, "Response of MG63 osteoblast-like cells to titanium and titanium alloy is dependent on surface roughness and composition," *Biomaterials,* vol. 19, no. 23, pp. 2219-2232, 1998.

[26] D.D. Deligianni, N. Katsala, S. Ladas, D. Sotiropoulou, J. Amedee, Y.F. Missirlis, "Effect of surface roughness of the titanium alloy Ti-6Al-4V on human bone marrow cell response and on protein adsorption," *Biomaterials,* vol. 22, no. 11, pp. 1241-1251, 2001.

[27] K. Anselme, P. Linez, M. Bigerelle, D. Le Maguer, A. Le Maguer, P. Hardouin, H.F. Hildebrand, A. Lost, J.M. Leroy, "The relative influence of the topography and chemistry of TiAl6V4 surfaces on osteoblastic cell behaviour," *Biomaterials,* vol. 21, no. 15, pp. 1567-1577, 2000.

[28] S.A. Naghibi, K. Raeissi, M.H. Fathi, "Corrosion and tribocorrosion behavior of Ti/TiN PVD coating on 316L stainless steel substrate in Ringer's solution," *Materials Chemistry and Physics,* vol. 148, pp. 614-623, 2014.

[29] N. Huang, P. Yang, Y.X. Leng, J. Wang, H. Sun, J.Y. Chen, G.J. Wan, "Surface modification of biomaterials by plasma immersion ion implantation," *Surface and Coatings Technology,* vol. 186, no. 1-2, pp. 218-226, 2004.

[30] A. Bagno, C. Di Bello, "Surface treatments and roughness properties of Ti based biomaterials," *Journal of Materials Science: Materials in Medicine,* vol. 15, no. 9, pp. 935-949, 2004.

[31] D.Q. Xiao, Z. Tan, C.D. Zhang, T.L. Guo, K. Duan, J. Weng, "Study on the microstructure and biocompatibility of inositol hexakisphosphate-modified titanium surface," *Materials Science Forum,* Vols. 809-810, pp. 507-513, 2015.

[32] K. Otsuka, C.M. Wayman, "Mechanism of shape memory effect and superelasticity," in *Shape Memory Materials*, Cambridge, UK, Cambridge University Press, 1998, pp. 27-26.

[33] S. Katayama, A. Matsunawa, A. Moritoma, S. Ishimoto, Y. Arata, in *EA Metzbower (Ed.), Proceedings of the Materials Processing Symposium, Laser Institute of America, Naval Research Department*, Washington, DC, 1983.

[34] H.C. Man, N.Q. Zhao, "Phase transformation characteristics of laser gas nitrided NiTi shape memory alloy," *Surface and Coatings Technology,* vol. 200, no. 18-19, pp. 5598-5605, 2006.

[35] D. Hoche, J. Kaspar, P. Schaaf, "Laser nitriding and carburization of materials," in *Laser surface engineering. Processes and applications*, Cambridge, U.K., Woodhead Publishing, 2015, pp. 33-58.

[36] P. Schaaf, J. Kaspar, D. Hoche, "Laser gas-assisted nitriding of Ti alloys," in *Comprehensive Materials Processing. Vol.9: Laser Machining and Surface Treatment*, Amsterdam, Elsevier, 2014, pp. 261-278.

[37] H.C. Man, M. Bai, F.T. Cheng, "Laser diffusion nitriding of Ti–6Al–4V for improving hardness and wear resistance," *Applied Surface Science,* vol. 258, pp. 436-441, 2011.

[38] A. Goransson, E. Jansson, P. Tengvall, A. Wennerberg, "Bone formation after 4 weeks around blood-plasma-modified titanium implants with varying surface topographies: an in vivo study," *Biomaterials,* vol. 24, pp. 197-205, 2003.

[39] T.M. Lee, E. Chang, C.Y. Yang, "Attachment and proliferation of neonatal rat calvarial osteoblasts on Ti6Al4V: effect of surface chemistries of the alloy," *Biomaterials,* vol. 25, pp. 23-32, 2004.

[40] R.J. Lazzara, T. Testori, P. Trisi, S.S. Porter, R.L. Weinstein, "Laser surface micro-texturing of Ti–6Al–4V substrates for improved cell integration," *Applied Surface Science,* vol. 253, pp. 7738-7743, 253.

[41] R. Hoehn, C. Hesse, H. Ince, M. Peuster, "First experience With the biostar-device for various applications in pediatric patients With congenital heart disease," *Catheterization and Cardiovascular Interventions,* vol. 75, no. 1, pp. 72-77, 2010.

[42] R. DesRoches, J. McCormick, M. Delemont, "Cyclic properties of superelastic shape memory alloy wires and bars," *Journal of Structural Engineering,* vol. 130, no. 1, pp. 38-46, 2004.

[43] T.E. Dye, An experimental investigation of the behavior of Nitinol, Switzerland: Virginia Tech, 1990.

[44] G. Airoldi, G. Riva, M. Vanelli, ""Superelasticity and shapememory memory effect in

NiTi orthodontic wires," in *Procceedings of the International Conference on Martensitic Transformations (ICOMAT'95)*, Lausanne, Switzerland, 1995.

[45] A. Kapanena, J. Ryhänenb, A. Danilova, J. Tuukkanena, "Effect of nickel–titanium shape memory metal alloy on bone formation," *Biomaterials,* vol. 22, no. 18, pp. 2475-2480, 2001.

[46] L.G. Machado, M.A. Savi, "Medical applications of shape memory alloys," *Brazilian Journal of Medical and Biological Research,* vol. 36, pp. 683-691, 2003.

[47] T.W. Duerig, A.R. Pelton, D. Stockel, "The use of superelasticity in medicine," *Metall-Heidelberg,* vol. 50, no. 9, pp. 569-574, 1996.

[48] D. Mantovani, "Shape memory alloys: Properties and biomedical applications," *The Journal of The Minerals, Metals & Materials Society (TMS),* vol. 52, no. 10, pp. 36-44, 2000.

[49] B. Li, L. Rong, Y. Li, V.E. Gjunter, "A recent development in producing porous Ni–Ti shape memory alloys," *Intermetallics,* vol. 8, no. 8, pp. 881-884, 2000.

[50] K. Wang, "The use of titanium for medical applications in the USA," *Materials Science and Engineering A,* vol. 213, no. 1-2, pp. 134-137, 1996.

[51] T.P. Schmalzried, J.J. Callaghan, "Current concepts review: wear in total hip and knee replacements," *The Journal of Bone & joint Surgery,* vol. 81, no. 1, pp. 115-136, 1999.

[52] H. Dong, T. Bell, "State-of-the-art overview: ion beam surface modification of polymers towards improving tribological properties," *Surface and Coatings Technology,* vol. 111, no. 1, pp. 29-40, 1999.

[53] D. Dowson, "A comparative study of the performance of metallic and ceramic femoral head components in total replacement hip joints," *Wear,* vol. 190, no. 2, pp. 171-183, 1995.

[54] D. Dowson, V. Wright, An Introduction to the Bio-mechanics of Joints and Joint Replacement, London, UK: Wiley-Blackwell , 1981.

[55] J. Black, G. Hastings, Handbook of Biomaterial Properties, London, UK: Chapman & Hall, 1998.

[56] D. Dowson, N.C. Wallbridge, "Laboratory wear tests and clinical observations of the penetration of femoral heads into acetabular cups in total replacement hip joints I : Charnley prostheses with polytetrafluoroethylene acetabular cups," *Wear,* vol. 104, pp. 203-215, 1985.

[57] J.F. Archard, "Contact and Rubbing of Flat Surfaces," *Journal of Applied Physics,* vol. 24, no. 8, pp. 981-988, 1953.

[58] C.R. Bragdon, D.O. O'Connor, J.D. Lowenstein, M. Jasty, W.D. Syniuta, "The importance of multidirectional motion on the wear of polyethylene," *Proceedings of the Institution of Mechanical Engineers, Part H: Journal of Engineering in Medicine,* vol. 210, no. 3, pp. 157-165, 1996.

[59] A. Wang, D.C. Sun, S.-S. Yau, B. Edwards, M. Sokol, A. Essner, V.K. Polineni, C. Stark, J.H. Dumbleton, "Orientation softening in the deformation and wear of ultra-high molecular weight polyethylene," *Wear,* Vols. 203-204, pp. 230-241, 1997.

[60] I.M. Hutchings, Tribology: Friction and Wear of Engineering Materials, London, UK: Edward Arnold, 1992.

[61] D. Dowson, Friction and wear of medical implants and prosthetic devices, ASM International, 1992.

[62] M.G. Perez, N.R. Harlan, F. Zapirain, F. Zubiri, "Laser nitriding of an intermetallic TiAl alloy with a diode laser," *Surface and Coatings Technology,* vol. 200, no. 16-17, pp. 5152-5159, 2006.

[63] Z. Liu, "Laser Applied Coatings," in *Reference Module in Materials Science and Materials Engineering*, UK, Elsevier, 2010, pp. 2622-2635.

[64] C. Hu, T.N. Baker, "The importance of preheat before laser nitriding a Ti–6Al–4V alloy," *Materials Science and Engineering: A,* vol. 265, no. 1-2, pp. 268-275, 1999.

[65] J. Kaspar, J. Bretschneider, S. Jacob, S. BonB, B. Winderlich, B. Brenner, "Microstructure, hardness and cavitation erosion behaviour of Ti–6Al–4V laser nitrided under different gas atmospheres," *Surface Engineering,* vol. 23, pp. 99-106, 2007.

[66] S. Mridha, T.N. Baker, "Effects of nitrogen gas flow rates on the microstructure and properties of laser-nitrided IMI318 titanium alloy (Ti–4V–6Al)," *Journal of Materials Processing Technology,* vol. 77, no. 1-3, pp. 115-121, 1998.

[67] A. Walker, J. Folkes, W.M. Steen, D.R.F. West, "Laser Surface Alloying of Titanium Substrates with Carbon and Nitrogen," *Surface Engineering,* vol. 1, no. 1, pp. 23-29, 1985.

[68] T. Bell, H.W. Bergmann, J. Lanagan, P.H. Morton, A.M. Staines, "Surface Engineering of Titanium with Nitrogen," *Surface Engineering,* vol. 2, no. 2, pp. 133-143, 1986.

[69] M.S. Selamat, T.N. Baker, L. mae Watson, "Study of the surface layer formed by the laser processing of Ti–6Al–4V alloy in a dilute nitrogen environment," *Journal of Materials Processing Technology,* vol. 113, no. 1-3, pp. 509-515, 2001.

[70] T.N. Baker, Laser surface modification of Ti alloys. In: Surface Engineering of Light Alloys - Aluminium, Magnesium and Titanium Alloys., Cambridge, UK: Woodhead Publications, 2010.

[71] L. Xue, M. Islam, A.K. Koul, M. Bibby, W. Wallace, "Laser Gas Nitriding of Ti-6Al-4V Part 2: Characteristics of Nitrided Layers," *Advanced Performance Materials,* vol. 4, no. 4, pp. 389-408, 1997.

[72] A. Zhecheva, W. Sha, S. Malinov, A. Long, "Enhancing the microstructure and properties of titanium alloys through nitriding and other surface engineering methods," *Surface and Coatings Technology,* vol. 200, no. 7, pp. 2192-2207, 2005.

[73] E. György, A. Pérez del Pino, P. Serra, J.L. Morenza, "Depth profiling characterisation of the surface layer obtained by pulsed Nd:YAG laser irradiation of titanium in nitrogen," *Surface and Coatings Technology,* vol. 173, no. 2-3, pp. 265-270, 2003.

[74] E. György, A. Pérez del Pino, P. Serra, J.L. Morenza, "Influence of the ambient gas in laser structuring of the titanium surface," *Surface and Coatings Technology,* vol. 187, no. 2-3, pp. 245-249, 2004.

[75] S. Yerramareddy, S. Bahadur, "The effect of laser surface treatments on the tribological behavior of Ti-6Al-4V," *Wear,* vol. 157, no. 2, pp. 245-262, 1992.

[76] O. Kubaschewski, E.L. Evans, Metallurgical thermochemistry, 5th ed., New York, USA: Pergamon Press, 1979.

[77] H.C. Man, Z.D. Cui, T.M. Yue, "Surface characteristics and corrosion behavior of laser

surface nitrided NiTi shape memory alloy for biomedical applications," *Journal of Laser Applications,* vol. 14, pp. 242-247, 2002.

[78] J. Antony, F. j. Antony, "Teaching the taguchi method to industrial engineers," *Work Study,* vol. 50, no. 4, pp. 141-149, 2001.

[79] V.C. Kumar, "Process parameters influencing melt profile and hardness of pulsed laser treated Ti–6Al–4V," *Surface and Coatings Technology,* vol. 201, pp. 3174-3180, 2006.

[80] A.K. Dubey, V. Yadava, , "Multi-objective optimization of Nd: YAG laser cutting of nickel-based superalloy sheet using orthogonal array with principal component analysis," *Optics and Lasers in Engineering,* Vols. 124-132, p. 46, 2008.

[81] G.S. Peace, Taguchi methods: a hands on approach, Harlow: Addison Wesley Publishing Com. Inc, 1992.

[82] C.H. Ng, C.W. Chan, H.C. Man, D.G. Waugh, J. Lawrence, "NiTi shape memory alloy with enhanced wear performance by laser selective area nitriding for orthopaedic applications," *Surface and Coatings Technology,* vol. 309, pp. 1015-1022, 2017.

[83] Q. Zhao, Y. Liu, E.W. Abel, "Effect of temperature on the surface free energy of amorphous carbon films," *Journal of Colloid and Interface Science,* vol. 280, no. 1, pp. 174-183, 2004.

[84] D.K. Owens, R.C. Wendt, "Estimation of the surface free energy of polymers," *Journal of Applied Polymer Science,* vol. 13, no. 8, pp. 1741-1747, 1969.

[85] D.Y. Kwok, A.W. Neumann, "Contact angle measurement and contact angle interpretation," *Advances in Colloid and Interface Science,* vol. 81, no. 3, pp. 167-249, 1999.

[86] T. Young, Miscellaneous Works of the Late Thomas Young, London, UK: John Murray, 1855.

[87] C.J. van Oss, M.K. Chaudhury, R.J. Good, "Monopolar surfaces," *Advances in Colloid and Interface Science,* vol. 28, pp. 35-64, 1987.

[88] C. Della Volpe, D. Maniglio, M. Brugnara, S. Siboni, M. Morra , "The solid surface free energy calculation. I. In defense of the multicomponent approach," *Journal of Colloid and Interface Science,* vol. 271, no. 2, pp. 434-453, 2004.

[89] S. Bhowmik, P. Jana, T.K Chaki, S. Ray, "Surface modification of PP under different electrodes of DC glow discharge and its physicochemical characteristics," *Surface and Coatings Technology,* vol. 185, no. 1, pp. 81-91, 2004.

[90] F.D. Blum, B. Metin, R. Vohra, O.C. Sitton, "Surface segmental mobility and adhesion - effects of filler and molecular mass," *The Journal of Adhesion,* vol. 82, no. 9, pp. 903-917, 2006.

[91] W. Shi, H. Dong, T. Bell, "Tribological behaviour and microscopic wear mechanisms of UHMWPE sliding against thermal oxidation-treated Ti6Al4V," *Materials Science and Engineering: A,* vol. 291, no. 1-2, pp. 27-36, 2000.

[92] H. Schmidt, A. Schminke, "Tribological behaviour of ion-implanted Ti6Al4V sliding against polymers," *Wear,* vol. 209, pp. 49-56, 1997.

[93] M.S. Phadke, Quality Engineering Using Robust Design, NJ, USA: Prentice Hall PTR Upper Saddle River, 1995.

[94] W.H. Yang, Y.S. Tarng, "Design optimization of cutting parameters for turning

operations based on the Taguchi method," *Journal of Materials Processing Technology,* vol. 84, no. 1-3, pp. 122-129, 1998.

[95] K. Venkatesan, R. Ramanujam, P. Kuppan, "Analysis of Cutting Forces and Temperature in Laser Assisted Machining of Inconel 718 Using Taguchi Method," *Procedia Engineering,* vol. 97, pp. 1637-1646, 2014.

[96] K.E. Freiberg, S. Bremer-Streck, M. Kiehntopf, M. Rettenmayr, A. Undisz, "Effect of thermomechanical pre-treatment on short- and long-term Ni release from biomedical NiTi," *Acta Biomaterialia,* vol. 10, no. 5, pp. 2290-2295, 2014.

[97] D. Yang, X. Lu, Y. Hong, T. Xi, D. Zhang, "The molecular mechanism for effects of TiN coating on NiTi alloy on endothelial cell function," *Biomaterials,* vol. 35, no. 24, pp. 6195-6205, 2014.

[98] T. Sun, N. Xue, C. Liu, C. Wang, J. He, "Bioactive (Si, O, N)/(Ti, O, N)/Ti composite coating on NiTi shapememory alloy for enhanced wear and corrosion performance," *Applied Surface Science,* vol. 356, pp. 599-609, 2015.

[99] H. Oettel, T. Bertram, V. Weihnacht, R. Wiedemann, S.V. Zitzewitz, "Mechanical behaviour of TiN coatings," *Surface and Coatings Technology,* vol. 97, pp. 785-789, 1997.

[100] American Society for Testing and Materials (ASTM) D7334–08, "Standard Practice for Surface Wettability of Coatings, Substrates and Pigments by Advancing Contact Angle Measurement," ASTM International, West Conshohocken, PA, 2013.

[101] E. Lugscheider, K. Bobzin, "The influence on surface free energy of PVD-coatings," *Surface and Coatings Technology,* Vols. 142-144, pp. 755-760, 2001.

[102] A. Galvin, C. Brockett, S. Williams, P. Hatto, A. Burton, G. Isaac, M. Stone, E. Ingham, J. Fisher, "Comparison of wear of ultra-high molecular weight polyethylene acetabular cups against surface-engineered femoral heads," *Journal of Engineering in Medicine,* vol. 222, no. 7, pp. 1073-1080, 2008.